https://dx.doi.org/10.1016/j.bioorg.2022.105863

Synthesis and biological evaluation of nusbiarylin derivatives as bacterial rRNA synthesis inhibitor with potent antimicrobial activity against MRSA and VRSA

Yangyi Qiu [a,1], Adrian Jun Chu [b,1], Tsz Fung Tsang [b], Yingbo Zheng [a], Nga Man Lam [b], Kendra Sek Lam Li [b], Margaret Ip [b], Xiao Yang [b,], Cong Ma [a,*]*

[a] State Key Laboratory of Chemical Biology and Drug Discovery, and Department of Applied Biology and Chemical Technology, The Hong Kong Polytechnic University, Kowloon, Hong Kong SAR, China

[b] Department of Microbiology, The Chinese University of Hong Kong, Prince of Wales Hospital, Shatin, Hong Kong SAR, China

ABSTRACT: Bacterial transcription is a valid but underutilized target for antimicrobial agent discovery because of its function of bacterial RNA synthesis. Bacterial transcription factors NusB and NusE form a transcription complex with RNA polymerase for bacterial ribosomal RNA synthesis. We previously identified a series of diarylimine and -amine inhibitors capable of inhibiting the interaction between NusB and NusE and exhibiting good antimicrobial activity. To further explore the structural viability of these inhibitors, coined “nusbiarylins”, 36 new derivatives containing diverse substituents at the left benzene ring of inhibitors were synthesized based upon isosteric replacement and the structure-activity relationship concluded from earlier studies. Some of the derivatives displayed good to excellent antibacterial efficacy

towards a panel of clinically significant pathogens including methicillin-resistance *Staphylococcus aureus* (MRSA) and vancomycin-resistance *S. aureus* (VRSA). In particular, compound **22r** exhibited the best antimicrobial activity with a minimum inhibitory concentration (MIC) of 0.5 μg/mL. Diverse mechanistic studies validated the capability of **22r** inhibiting the function of NusB protein and bacterial rRNA synthesis. *In silico* study of drug-like properties also provided promising results. Overall, this series of derivatives showed potential antimicrobial activity and drug-likeness and provided guidance for further optimization.

Keywords: Bacterial transcription, protein-protein interaction, antibacterial activity, MRSA

1. Introduction

Antimicrobial resistance (AMR) causes re-emerging epidemics of infectious diseases threating human health and global economy. Unprecedented drug classes and mechanisms of action are urgented required to combat AMR. Bacterial transcription is a valid but underutilized target for the discovery of antimicrobial agents [1]. Multiple transcription factors interact with RNA polymerase (RNAP) to regulate bacterial transcription, where the protein-protein interactions (PPIs) in bacterial transcription are essential for cell viability and can serve as basis for rational antimicrobial drug design, as targeting PPIs represents an effective strategy to minimize generation of bacterial resistance [2]. Additionally, using these unique antimicrobial targets with novel pharmacological mechanisms for antimicrobial drug discovery will thus be able to

overcome antimicrobial resistance of current antibiotics applied in clinics.

Bacterial transcription factors NusB and NusE particularly attracted our attention [3]. These two small proteins are highly conserved and exclusively exist in bacteria [4, 5]. They bind to each other to form a bacterial transcription complex with RNAP (Figure 1A) [6], which is responsible for bacterial rRNA synthesis [7, 8]. Studies showed that the function of PPI between NusB and NusE highly correlated to bacterial cell viability [9, 10], which may serve as an appropriate target for novel antimicrobial agent discovery (Figure 1B) [1].

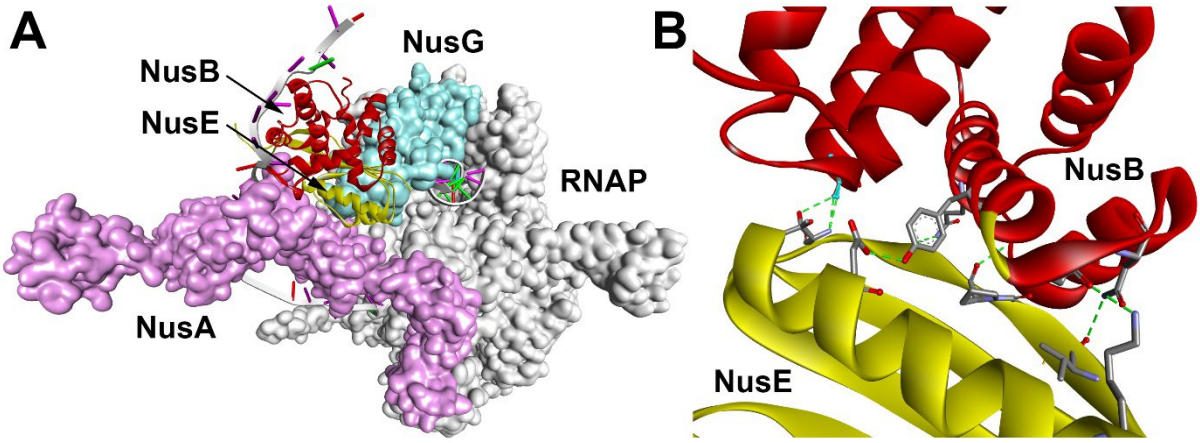

Figure 1. (A) Bacterial transcription complex formed by RNAP (Grey), NusB (Red), and NusE (yellow), NusA (pink), NusG (cyan), and RNA (PDB 6TQN, [11]); (B) Interaction between NusB (red) and NusE (yellow) (PDB 3D3B, [12])

In previous studies, we chose four important interctions of amino acid residues between NusB and NusE to design a pharmacophore model for virtual screening and discovered a hit compound **MC4-1** (Figure 2) [13]. The following biological evaluations on **MC4-1** and a series of diarylimine and –amine compounds derivatized from **MC4-1** demonstrated the inhibitory activity of interrupting bacterial ribosomal RNA synthesis, and broad-spectrum antimicrobial activity against a panel of clinically significant pathogens including a wide range of methicillin-

resistance *S. aureus* (MRSA) strains, with minimum inhibitory concentration (MIC) values as low as 1 μg/mL [14, 15]. We named this class of compounds nusbiarylins by using the target NusB as the prefix and biaryl structure as the suffix [15]. Additionally, these compounds displayed capability of inhibiting bacterial toxin release [16], together with inhibitors of PPI between bacterial RNA polymerase and sigma factor [17-19], which signified the potential of bacterial transcription inhibitors in antimicrobial drug discovery.

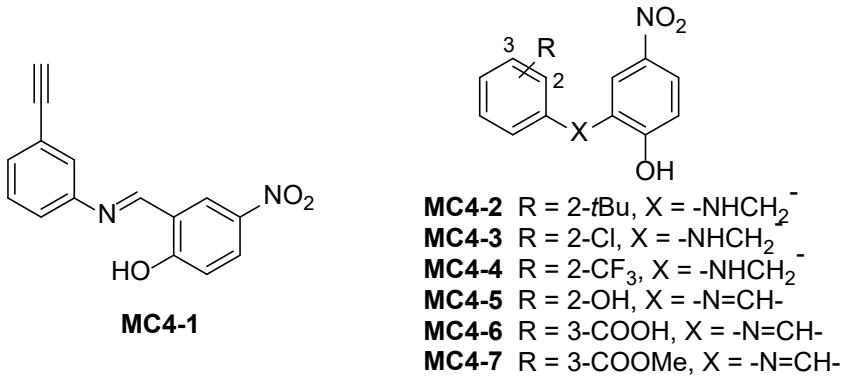

Figure 2. Chemical structures of hit compound MC4-1 and its potent derivatives.

The preliminary SAR concluded from these nusbiarylin compounds revealed that introduction of substituents into the left benzene ring of compounds improved antibacterial activity and demonstrated great tolerance to both hydrophobic and hydrophilic functional groups. Specifically, the 2-*t*-butyl (**MC4-2**), 2-chloro (**MC4-3**) and 2-trifluoromethyl (**MC4-4**) substituted derivatives showed great antibacterial activity against *S.aureus* ATCC 25923 with MIC values ranging between 1-4 μg/mL (Figure 2). Interestingly, analogues containing hydroxyl (**MC4-5**), carboxylic acid (**MC4-6**) or ester group (**MC4-7**) also displayed great antibacterial potency (MIC 2-4 μg/mL). Based on the structure-based protein-ligand docking of **MC4-2** and **MC4-6** to NusB (Figure 3), the amino acid residues at the binding site of NusB

can form a small pocket that is able to accommodate diverse substituents on the left benzene of compounds. We hypothesized that slight improvement on the antimicrobial activity of hydrophobic group substituted derivatives may be credited to the greater lipid bilayer permeability but both hydrophobic and hydrophilic groups were acceptable by fitting into this pocket. In order to achieve an in-depth understanding of the adaptability of substituent types at the left benzene ring, it is highly desirable to generate novel derivatives containing unprecedented hydrophilic and hydrophobic groups substituted at the core structure of lead compound.

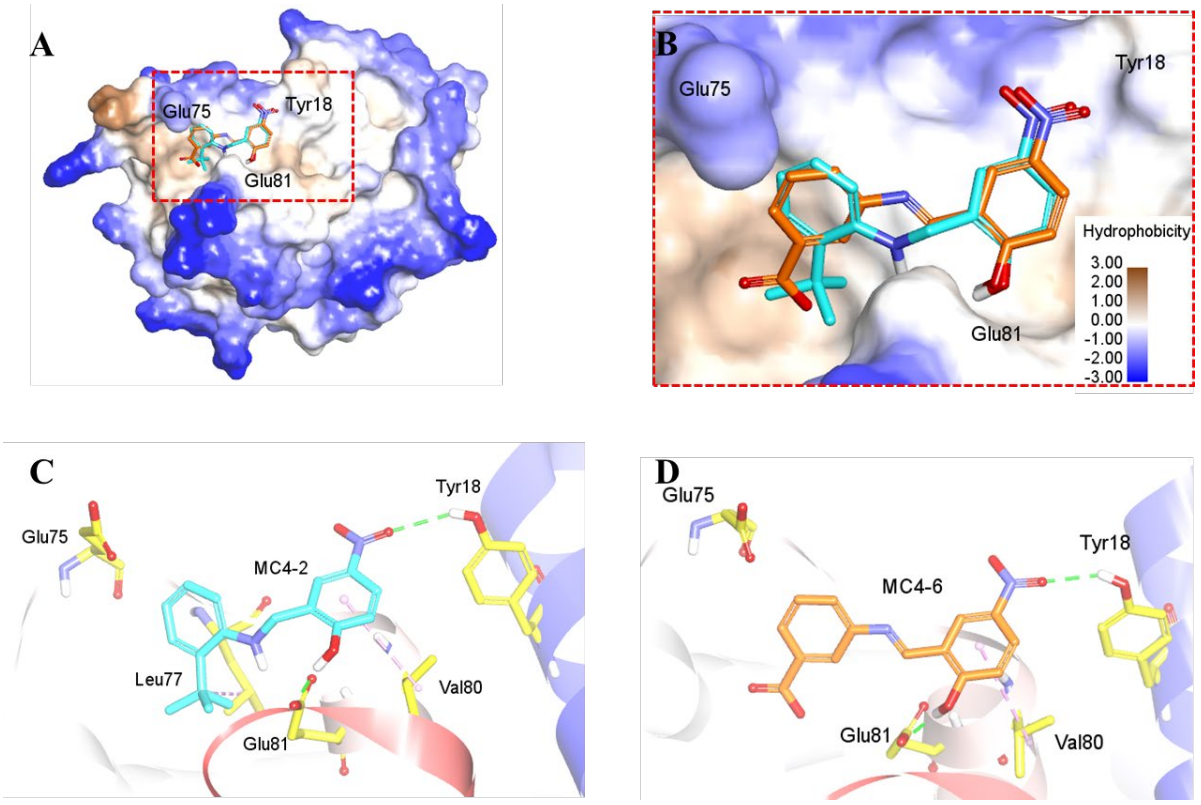

Figure 3. (A) Docking models of compound **MC4-2** (cyan) and **MC4-6** (orange) with NusB (PDB: 3D3B) by Discovery Studio 2016. (B) Enlarged region of the binding pocket for **MC4-2** and **MC4-6** with the hydrophobicity of NusB surface colored in brown and three hot-spot residues Glu75, Glu81, and Tyr18 labeled. Detailed interactions of **MC4-2** (C) and **MC4-6** (D) with NusB: hydrogen bonding interactions (green), and hydrophobic interactions (pink).

It is well established that bioisosteric replacement plays a major role in the search for analogues of an active molecule with the aim of improving its pharmacological profiles. It requires substitution of one atom or group of atoms in the parent compound by another, with similar physicochemical properties [20]. In this study, we intended to extend our earlier studies by identifying innovative carboxylic acid bioisosteres for left benzene substituted derivatives with improved antibacterial profiles based upon previous SAR and rational design. In light of promising antibacterial potency of compounds **MC4-2**, **MC4-3**, and **MC4-4** containing hydrophobic substituents at the left benzene ring, several new analogues with diverse hydrophobic moiety were also synthesized for testing antimicrobial activity.

2. Chemistry

2.1 Derivative Design

Carboxyl group can be a crucial constituent of a pharmacophore and is successfully applied in more than 450 marketed drugs [21], including widely used β-lactam antibiotics, nonsteroidal anti-inflammatory drugs and statins [22]. However, the presence of carboxyl group in drug molecules may also be responsible for undesired attributes, such as limited permeability across biological membranes, metabolic instability as well as potential idiosyncratic toxicities [23]. To avoid such drawbacks, especially the diminished permeability, isosteric replacement is a classical strategy in medicinal chemistry. In view of the promising inhibitory activity of compound **MC4-6** with 3-COOH, typical surrogates of carboxyl group such as sulfonamides,

amides, hydroxamic esters, substituted phenols, and oxazolidinediones were introduced at 3-position in an attempt to increase its permeability and thus improve its antibacterial activity. On the other side, hydrophobic substituents such as nitriles, phenyl and substituted phenyl groups replacing previously installed simple alkyl and halide groups at the left benzene ring provided a series of novel derivatives to probe the binding pocket. These groups generally display great protein binding affinity [21]. Their antibacterial activity was also examined.

2.2 Synthesis

Synthesis of the target compounds **21a-22r, 22a-22r** is shown in Scheme 1. Reaction of 5-nitrosalicylaldehyde **1** with diverse anilines **2-20** in ethanol at room temperature provided imine **21a-21r** in 78-93% yields. The corresponding amine compounds **22a-22r** were prepared *via* reductive amination in 76-93% yields.

Scheme 1. Synthesis of target compounds **21a-21r** and **22a-22r**[a]

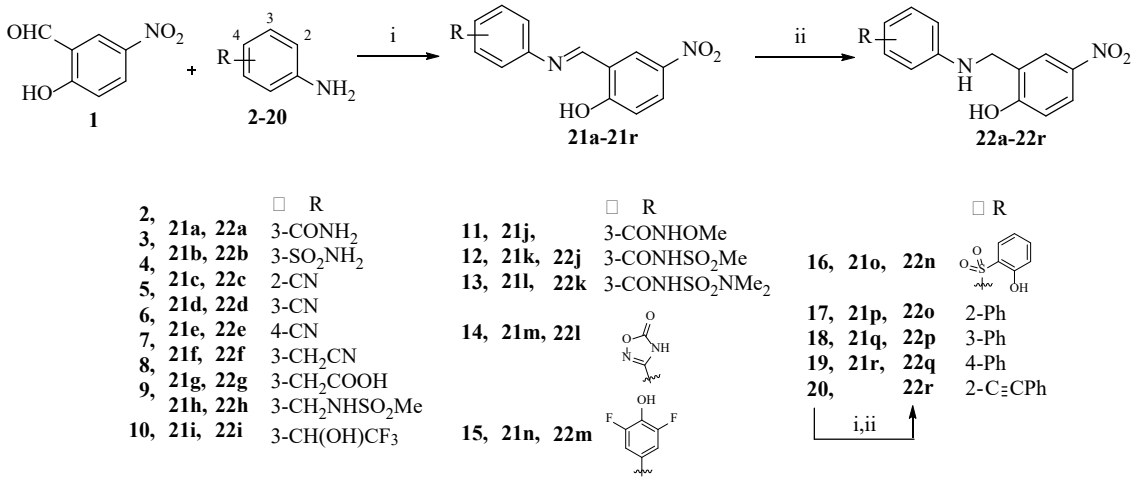

[a]Reagents and conditions: (i) EtOH, rt, overnight, 78-93%; (ii) $NaBH(OAc)_3$, DCM, rt, overnight, 76-93%.

Sulfonamide intermediate **9** was obtained in two steps starting from the reaction between benzaldehyde **23** and methanesulfonamide, followed by reduction of the nitro group (Scheme 2a) [24]. The ketone intermediate **10** was prepared from trifluoroacetophenone **25** through nitration in 74% yield, followed by reduction of ketone and nitro using sodium borohydride and iron power, respectively (Scheme 2b).

Hydroxamic acid ester and *N*-sulfonylcarboxamide intermediates **11-13** were synthesized from *tert*-butyloxycarbonyl (Boc)-protected 3-amino benzoic acid **28** through condensation reactions, followed by deprotection of the Boc group using trifluoroacetic acid (TFA) (Scheme 2c).

Oxadiazol-5(4*H*)-one intermediate **14** was synthesized from 3-aminobenzonitrile **5** following the described procedure (Scheme 2d) [25, 26]. With respect to substituted phenol intermediates **15** and **16**, the former was obtained by coupling *O*-allyl protected bromobenzene **35** with (3-nitrophenyl)boronic acid **36** under Suzuki reaction conditions, followed by reduction of nitro group (Scheme 2e), while the latter was synthesized starting from the coupling of 1-bromo-3-nitrobenzene **38** and 2-methoxybenzenethiol **39**, followed by hydrolysis of methyl ether and reduction of nitro group (Scheme 2f). Intermediate **20** was readily prepared from 2-iodoaniline **42** under Sonogashira reaction conditions in 91% yield (Scheme 2g).

Scheme 2. Synthesis of intermediate compounds **9-16, 20**[a]

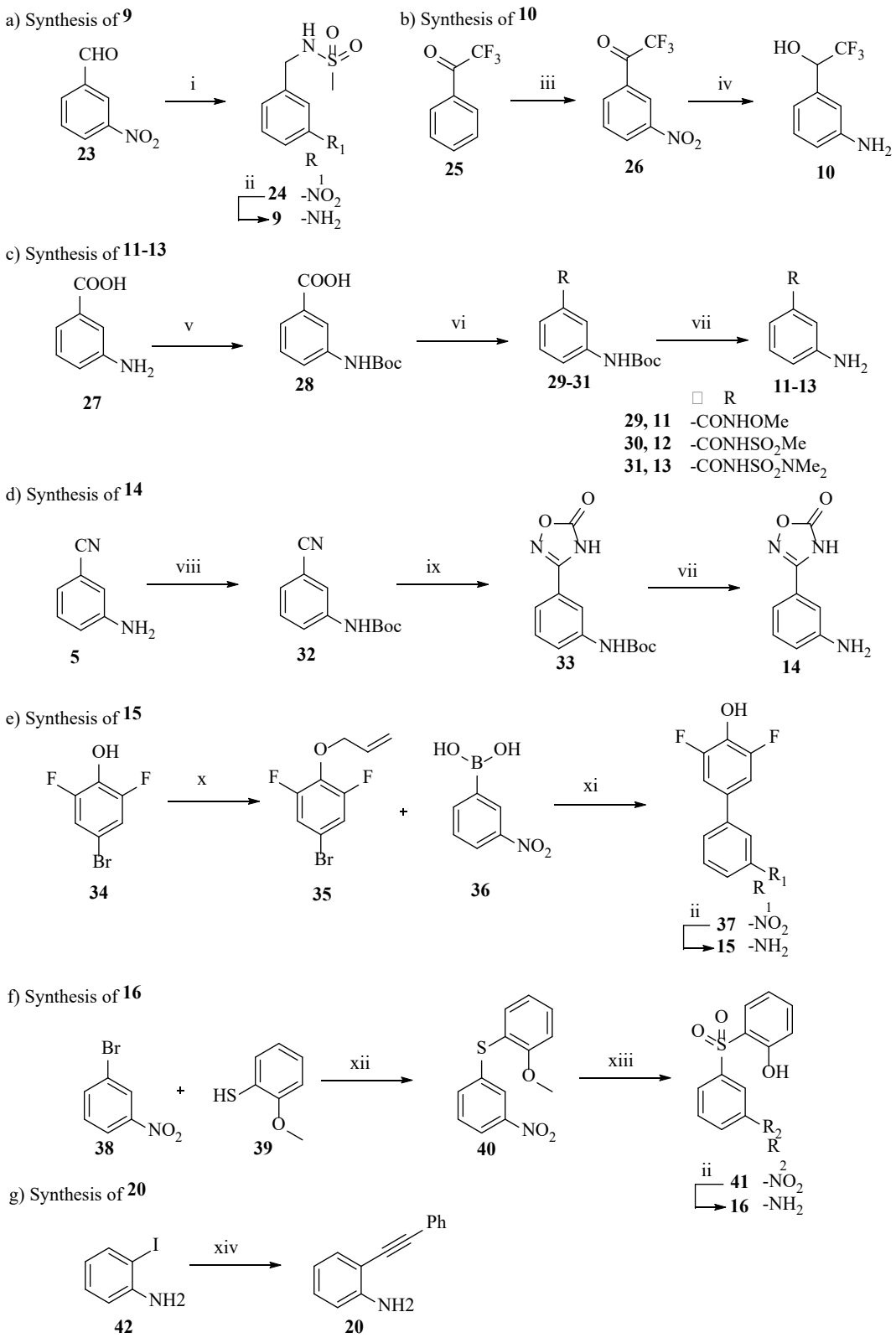

[a]Reagents and conditions: (i) methanesulfonamide, titanium(IV) ethoxide, toluene, 110 °C, 4 h; then $NaBH_4$, THF/MeOH, rt, 3 h, 69% in two steps; (ii) iron, NH_4Cl, EtOH/water, 80 °C, 1

h, 76-86%; (iii) KNO_3, conc. H_2SO_4, 0 °C, 74%, (iv) $NaBH_4$, EtOH, rt, 1h; then iron, NH_4Cl, EtOH/water, 80 °C, 1 h, 84% in two steps; (v) $(Boc)_2O$, TEA, dixoane/water, rt, 4 h, 90%; (vi) EDCI, DMAP, DIEA, methoxyammonium chloride for **11**, methanesulfonamide for **12**, or N,N-dimethylsulfamide for **13**, DCM, rt, overnight, 67-73%; (vii) TFA, DCM, rt, 3 h, 85-92%; (viii) $(Boc)_2O$, EtOH, rt, overnight, 87%; (ix) hydroxylamine hydrochloride, TEA, EtOH, 80 °C, 3 h; then 2-ethylhexyl chloroformate, pyridine, 0 °C, 30 min; then xylene, 140 °C, 49% in three steps; (x) allyl bromide, K_2CO_3, 60 °C, 3 h, 65%; (xi) $Pd(PPh_3)_4$, K_3PO_4, DMF/water, 100 °C, 18 h, 71%; (xii) $Pd_2(dba)_3$, Xantphos, DIEA, dioxane, 100 °C, 6 h, 76%; (xiii) mCPBA, DCM, rt, 1 h; then $AlCl_3$, DCM, rt, 1 h, 71% in two steps; (xiv) $PdCl_2(PPh_3)_2$, CuI, TEA, phenylacetylene, THF, rt, overnight, 91%.

3. Results and discussion

3.1 Antimicrobial activity

Antimicrobial activity screening of target compounds **21a-21r** and **22a-22r** against *S. aureus* type strain ATCC® 25923 was performed by broth microdilution method following guidelines as stipulated by the Clinical & Laboratory Standards Institute (CLSI) and the results shown in Table 1 [27].

In concordance with our hypothesis, all carboxylic acid isosteric substitution in imine-linked derivatives **21a-21o** led to equal or slightly superior antimicrobial activities (MIC 2-4 μg/mL) compared to the 3-COOH substituted parent compound **MC4-6** (MIC 4 μg/mL). Among them, sulfonamide **21b**, phenylacetic acid **21g**, alcohol **21i**, and phenol **21n** exhibited the highest activities with MIC values of 2 μg/mL. Other bioisosteric derivatives showed equal potency to

the parent compound **MC4-6**, with MIC values of 4 μg/mL. Compounds **21p-21r**, all with MIC values of 8 μg/mL, appeared to inhibit bacterial growth albeit to slightly lesser extent than the previously synthesized analogues containing other hydrophobic substituents on the left benzene group [14, 15]. These results, along with our previous observations regarding SAR, demonstrated that apart from hydrophobic groups, introduction of appropriate hydrophilic moieties on the left benzene ring of imine-linked nusbiarylin derivatives can improve their antimicrobial activities, suggesting high potential for diverse surrogate structures.

When the rigid imine linker was reduced to the flexible amine, derivatives **22a-22n** displayed decreased antimicrobial activities compared to their imine analogues. Notably, compounds **22j**, **22k**, and **22m** still maintained antimicrobial activity, while other amine analogues showed drastically decreased activities. When compared to the imine compounds with hydrophilic substituents possessing good inhibitory activities (MIC 2-4 μg/mL), the results suggested that hydrophilic substituents may not be compatible with the amine linker. In contrast, compounds **22o-22q** with phenyl group on the left benzene ring showed enhanced potency with MIC values of 1 μg/mL. When we extended the phenyl substituent by the ethyne group as in compound **22r**, it displayed excellent antimicrobial activity with an MIC value of 0.5 μg/mL. The results again demonstrated previous observations and the compatibility of hydrophobic substituents over hydrophilic ones with the amine linker regarding the antimicrobial activity of inhibitors.

Table 1. Antibacterial activities of compounds **21a-21r** and **22a-22r**.

Structure	No.	R	MIC (μg/mL)[a]
	21a	3-$CONH_2$	4
	22a		>256
	21b	3-SO_2NH_2	2
	22b		>256

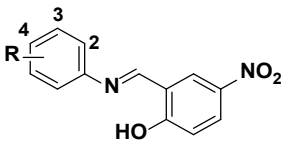

21a-21r

21c **22c**	2-CN	2 16
21d **22d**	3-CN	4 >256
21e **22e**	4-CN	4 64
21f **22f**	3-CH_2CN	4 128
21g **22g**	3-CH_2COOH	2 >256
21h **22h**	3-CH_2NHSO_2Me	4 8
21i **22i**	3-$CH(OH)CF_3$	2 16
21j	3-CONHOMe	4
21k **22j**	3-$CONHSO_2Me$	4 >256
21l **22k**	3-$CONHSO_2NMe_2$	4 >256
21m **22l**	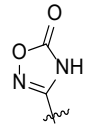	4 >256
21n **22m**	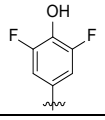	2 8
21o **22n**	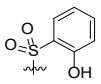	4 64
21p **22o**	2-Ph	8 1
21q **22p**	3-Ph	8 2
21r **22q**	4-Ph	8 1
22r	2-C≡CPh	0.5

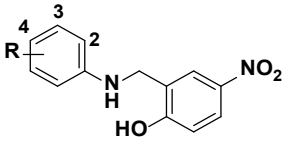

22a-22r

[a] MIC values against *S. aureus* ATCC® 25923.

We then examined the antibacterial spectra of these compounds. The bacterial panel we used consisted of 6 pathogens on most recent "WHO priority pathogens list for guiding R&D of new antibiotics" consisting of three Gram-positive species: *Enterococcus faecalis*, *S. aureus*,

Streptococcus pneumonia; and three Gram-negative bacteria: *Acinetobacter baumannii*, *Pseudomonas aeruginosa*, and *Enterobacter* spp.. A CLSI-based broth microdilution method was employed for antibiotic susceptibility testing, and the results were shown in Table 2. In general, the compounds demonstrated broad-spectrum antimicrobial activity against both Gram-positive and -negative bacteria. Additionally, these compounds displayed specific activities against the Gram-positives *S. aureus*, *S. pneumonia*, and *E. faecalis*. While some compounds also displayed mild antibacterial activity against *A. baumannii* over other less responsive Gram-negative pathogens, this suggests that Gram-positive bacteria may be more susceptible to these compounds in general. Given that *A. baumannii* tops the WHO priority pathogens list with urgent requirements for new antibiotics to be developed, this presents a intriguing prospect where, through structural optimisations, our compounds may be further developed into novel antimicrobial agents to combat specific Gram-negative strains. In contrast, other Gram-negative bacteria tested appeared less susceptible to treatment by the compounds, which may generally be attributable to reduced cell permeability and presence of multidrug efflux mechanisms, and that surmounting such obstacles possibly requires modifications to their chemical structures and further investigations.

Table 2. Antimicrobial activities of compounds **21a-21r** and **22a-22r** against 7 representative bacterial strains in the WHO priority pathogens list for guiding R&D of new antibiotics.

No.	*E. faecalis*	*S. aureus*[a]	*S. aureus*[b]	*S. pneumoniae*	*A. baumannii*	*P. aeruginosa*	*E. cloacae*

21a	>256	4	16	8	128	>256	>256
21b	>256	2	16	16	128	>256	>256
21c	>256	2	8	64	128	>256	>256
21d	>256	4	16	16	128	>256	>256
21e	>256	4	16	64	256	>256	>256
21f	>256	4	16	16	128	>256	>256
21g	>256	2	16	16	128	>256	>256
21h	256	1	8	16	128	>256	>256
21i	>256	2	8	16	128	>256	>256
21j	>256	4	16	16	128	>256	>256
21k	>256	4	16	128	256	>256	>256
21l	>256	4	16	32	128	>256	>256
21m	>256	1	8	16	128	>256	>256
21n	>256	2	8	32	>256	>256	>256
21o	256	4	64	32	256+	>256	>256
21p	256	8	32	32	>256	>256	>256

21q	>256	8	16	128	256	>256	>256
21r	64	8	64	64	256	>256	>256
22a	>256	>256	>256	>256	>256	>256	>256
22b	>256	>256	>256	>256	>256	>256	>256
22c	64	4	32	64	>256	>256	>256
22d	>256	>256	>256	>256	>256	>256	>256
22e	128	64	32	128	256	>256	>256
22f	256	32	128	128	>256	>256	>256
22g	>256	>256	>256	>256	>256	>256	>256
22h	>256	8	64	256	>256	>256	>256
22i	>256	16	64	64	>256	>256	>256
22j	>256	>256	>256	>256	>256	>256	>256
22k	>256	>256	>256	>256	>256	>256	>256
22l	>256	>256	>256	256	>256	>256	>256
22m	32	8	16	8	>256	>256	>256
22n	128	64	64	64	>256	>256	>256

22o	4	1	1	4	>256	>256	>256
22p	8	2	2	4	>256	>256	>256
22q	8	1	2	8	>256	>256	>256
22r	0.5	0.5	0.5	1	>256	>256	>256
Vancomycin	1	2	2	1	>64	>64	>64
Oxacillin	32	1	1	2	>64	>64	≥64
Gentamicin	16	0.5	2	16	32	2	1
Ciprofloxacin	4	2	2	2	1	0.5	≤0.0625

E. faecalis : *Enterococcus faecalis* ATCC® 19433, *S. aureus*[a]: *S. aureus* ATCC® 25923, *S. aureus*[b]: *S. aureus* ATCC® 29213, *S. pneumoniae* : *Streptococcus pneumoniae* ATCC® 49619, *A. baumannii* : *Acinetobacter baumannii* ATCC® 19606, *P. aeruginosa* : *Pseudomonas aeruginosa* ATCC® 27853, *E. cloacae* : *Enterobacter cloacae* ATCC® 13047, VAN: vancomycin, OXA: oxacillin, GEN: gentamicin, CIP: ciprofloxacin.

MRSAs represent some of the most prevalent multidrug-resistant bacteria worldwide, where some strains – such as vancomycin-resistant *S. aureus* (VRSA) – have even developed

resistance to “last-resort” antibacterial chemotherapeutants currently available in the market. We therefore also tested our compounds against a series of representative clinically isolated lineages of hospital-acquired (HA-) and community-associated (CA-) MRSAs, as well as VRSA strains. The MRSA strains include: HA-MRSA clone ST-239 prevalent in Asian countries, the epidemic Brazilian/Portuguese clone ATCC® BAA-43, the epidemic Iberian clone ATCC® BAA-44, and the ST-45 clones which spread across Germany, the Netherlands and Ontario, Canada over the past decade; CA-MRSA clone ST-30 and ST-59 prevalent in Hong Kong and Asian countries, the major North American and European clone USA300, clone ST-22 emerging in the Indian subcontinent, and the hypervirulent community-acquired but methicillin-susceptible US strain MSSA-476; laboratory strains of known resistant mechanisms such as isolate SA-1199B for fluoroquinolone resistance [28], SA-RN4220-pUL5054 for macrolide resistance [29], as well as three classes of aminoglycoside-modifying enzymes (AMEs) SA-APH2”-AAC6’, SA-APH3’ and SA-ANT4’ for aminoglycoside resistance [30].

As shown in Table 3, all 3 selected compounds displayed fairly good to excellent antibacterial activity against the tested MRSA strains, with efficacy on par with that elicited by vancomycin. Some strains were resistant to oxacillin – the current first-line antibiotic used in the USA for treatment of MRSA infections – as well as other common drug choices such as the protein-synthesis inhibitor gentamicin. In all cases of individual resistance mechanisms harboured by clinical strains, they all responded to treatment by our compounds, suggesting little to no overlap in their modes of action. Our compounds were able to maintain stable MIC values against a wide range of MRSA strains, suggesting the compounds may be further developed to

treat infections caused by MRSAs.

Table 3. Antimicrobial activity evaluation of compounds **22o**, **22q**, and **22r** against representative globally spread HA- and CA-MRSA strains.

	22o	**22q**	**22r**	Van	Gen	Oxa
HA-MRSA ST239	2	256	0.5	1	>64	>64
ATCC BAA-43	1	4	0.5	2	>64	>64
ATCC BAA-44	2	4	0.5	2	>64	>64
HA-MRSA ST45	2	4	0.5	1	32	8
CA-MRSA ST30	2	8	0.5	1	1	32
CA-MRSA ST59	2	4	0.5	1	1	32
CA-MRSA USA300	8	16	2	1	2	>64
CA-MRSA ST22	4	16	1	0.5	2	>64
MSSA 476 BAA-1721	4	256	2	1	1	2
SA-1199B	4	16	2	1	4	4
SA-RN4220-pUL5054	2	8	0.5	1	1	0.5
SA-APH2"-AAC6'	4	16	1	1	>64	>64

SA-APH3'	4	8	0.5	1	0.5	2
SA-ANT4'	4	16	1	2/1+	>64	>64

Van: vancomycin, Oxa: oxacillin, Gen: gentamicin.

The VRSA strains used were provided by the Network on Antimicrobial Resistance in *S. aureus* (NARSA) for distribution by BEI Resources, NIAID, NIH and administered by ATCC (Manassas, Virginia, United States), which include: VRSA-1 (NR-46410 / *S. aureus* strain HIP11714), VRSA-2 (NR-46411 / *S. aureus* strain HIP11983), VRSA-3a (NR-46412 / *S. aureus* strain HIP13170), VRSA-3b (NR-46413 / *S. aureus* strain HIP13419), VRSA-4 (NR-46414 / *S. aureus* strain HIP14300), VRSA-5 (NR-46415 / *S. aureus* strain HIP15178), VRSA-6 (NR-46416 / *S. aureus* strain AIS 2006032), VRSA-7 (NR-46417 / *S. aureus* strain AIS 2006045), VRSA-8 (NR-46418 / *S. aureus* strain 71080), VRSA-9 (NR-46419 / *S. aureus* strain AIS 080003), VRSA-10 (NR-46420 / *S. aureus* strain AIS 1000505), VRSA-11a (NR-46421 / *S. aureus* strain AIS 1001095), VRSA-11b (NR-46422 / *S. aureus* strain AID 1001123).

As shown in Table 4, all 3 selected compounds displayed remarkable antibacterial activity against the tested VRSA strains, where in contrast most strains were evidently resistant towards or desensitized for vancomycin as well as oxacillin, both of which are inhibitors of bacterial cell wall synthesis. Our compounds appeared to be effective against an array of VRSA strains harbouring multiple mechanisms of drug resistance, which strongly supports their clinical prospect and warrants further development as potential new treatment options against

increasingly untenable and serious infections caused by VRSAs.

Table 4. Evaluating antimicrobial activity of compounds **22o**, **22q**, and **22r** against representative panel of VRSA strains obtained from NARSA through BEI Resources.

	22o	**22q**	**22r**	Van	Gen	Oxa
VRSA-1	≤0.25	2	≤0.25	>256	64	>256
VRSA-2	1	2	≤0.25	128	64	>256
VRSA-3a	1	4	≤0.25	64	>64	256
VRSA-3b	2	4	0.5	>256	>64	>256
VRSA-4	2	4	0.5	>256	4	256
VRSA-5	2	4	≤0.25	256	4	128
VRSA-6	2	4	0.5	>256	>64	64
VRSA-7	2	4	0.5	>256	>64	256
VRSA-8	2	4	0.5	>256	64	>256
VRSA-9	4	8	1	>256	>64	>256
VRSA-10	4	8	1	>256	8	>256
VRSA-11a	4	4	0.5	>256	32	1

VRSA-11b	4	8	1	>256	32	32

Van: vancomycin, Oxa: oxacillin, Gen: gentamicin.

3.2 Time-kill kinetics and ATP production

To study the time- and dose-dependent relationship between our nusbiarylins and bacterial viability, compound **22r** was added to *S. aureus* ATCC® 25923 and USA300 at folds relative to their initial MICs. Compound **22r** showed largely bacteriostatic trends against both *S. aureus* strains over the course of 6 h, with marked descends in CFU counts to levels beyond detection limit observed only at the highest concentrations (Figure 4).

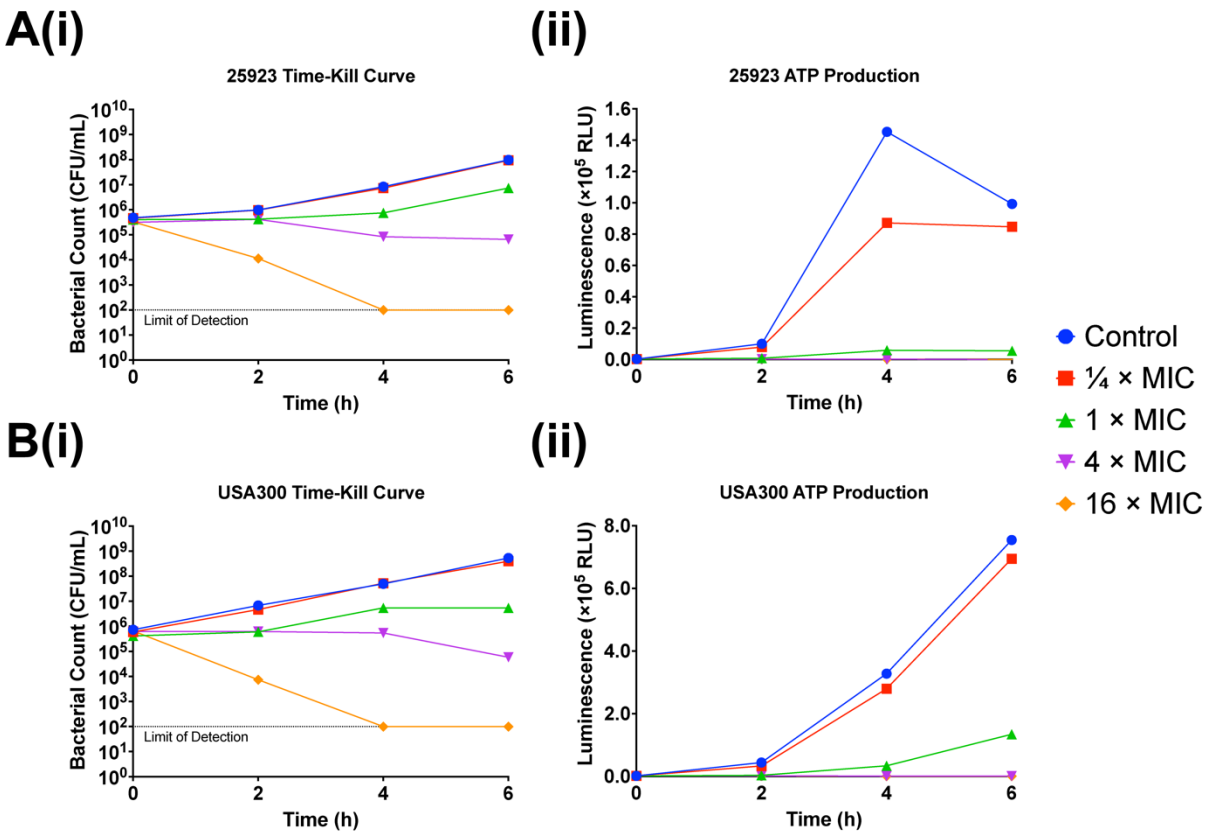

Figure 4. Effects of compound **22r** on the (i) time-kill kinetics and (ii) ATP production of (A) *S. aureus* ATCC® 25923 and (B) CA-MRSA strain USA300 at ¼, 1, 4 and 16 MIC in Mueller-Hinton broth (MHB) media. Experiments were performed in triplicates. 25923: *S. aureus* ATCC® 25923; USA300: CA-MRSA strain USA300.

As one of the defining traits of antibiotic efficacy is the arrest of cellular respiration [31], ATP production rate of both *S. aureus* strains was also closely monitored in tandem with each time-kill kinetics assay time points using identical experimental setups and samples. At 4 h, significant decreases in *S. aureus* ATCC® 25923 ATP production rate compared to untreated control group began to manifest at ¼ MIC of compound **22r**. As concentrations of compound **22r** increased, cellular respiration of the staphylococcal type strain was significantly suppressed. In USA300, only a mild decrease in ATP production rate was observed at ¼ MIC of compound **22r** compared to untreated control, with higher concentrations eliciting more pronounced inhibitory effects on respiration. The results were consistent with previously reported trends demonstrated by the bacterial transcription inhibitor class drug rifampicin, where efficacy of such antimicrobials is inversely correlated to rate of respiration in target organism [32, 33].

3.3 Study of antimicrobial resistance

As PPI inhibitors theoretically minimize the generation of antimicrobial resistance [2], the

emergence of resistance in *S. aureus* ATCC® 25923 was assessed through repeated exposure to sub-inhibitory concentrations of representative nusbiarylin compound **22r** consecutively for 12 days. As shown in Figure 5, no antimicrobial resistance was observed on *S. aureus* treated by **22r** (generation of resistance was defined by greater than 4 fold increase in MIC). Since the generation of resistance is a major concern for novel antimicrobial compounds, the result implied the potential of nubiarylins for further antimicrobial drug development.

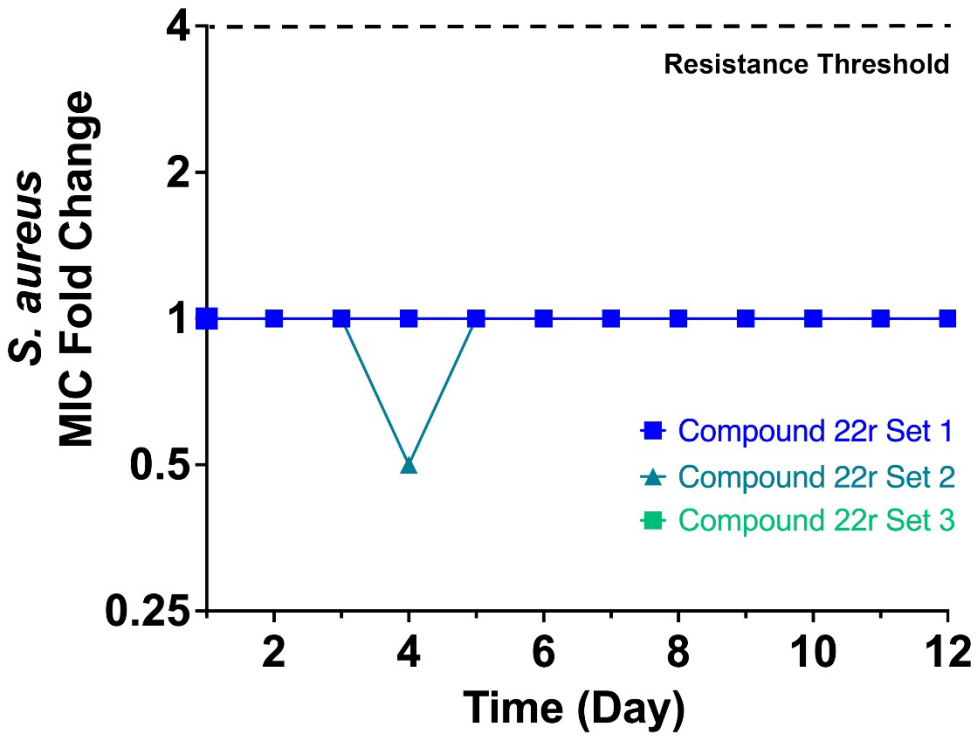

Figure 5. Serial passage of **22r** in *S. aureus* ATCC25923.

3.4 Changes of major cellular macromolecules

To investigate the effects of our nusbiarylins on the levels of DNA, RNA and protein production, type strain *S. aureus* ATCC® 25923 cells were treated with compound **22r** along side with

the transcription inhibitor rifampicin as the control drug at sub-inhibitory concentrations. Both of the antimicrobial agents were added at ¼ and ⅛ MIC respectively at the end of lag phase (OD_{600} = 0.2) and staphylococcal cells were subsequently harvested upon reaching mid-exponential phase (OD_{600} = 0.6), after which major macromolecules were extracted and the levels of total DNA, RNA and protein were quantified. Total levels of DNA in *S. aureus* were not markedly affected by either treatment compared to untreated control (Figure 6 DNA). Total levels of RNA in *S. aureus* were significantly reduced when cultured in the presence of ⅛ MIC of both rifampicin and compound **22r**, which is consistent with previous observations attributable to the known mechanisms of action of rifampicin and that of previously reported nusbiarylins (Figure 6 RNA). Protein levels largely corresponded to that of RNA levels (Figure 6 Protein). The results present compound **22r** as a promising antimicrobial with the capacity to impede bacterial RNA synthesis at similar extent as the class drug rifampicin.

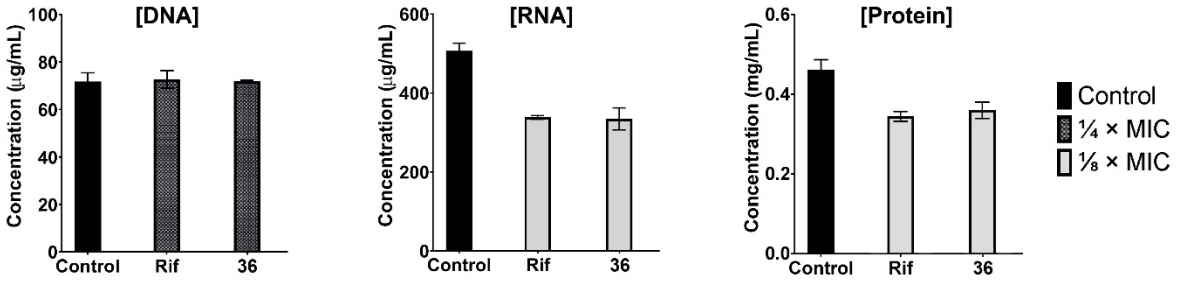

Figure 6. Quantification of levels of total DNA, total RNA and total protein in *S. aureus* ATCC® 25923 cells treated by rifampicin (Rif) and compound **22r** at sub-MIC doses.

3.5 Real-time qPCR of rRNA expression

Given their role as ribosomal RNA-targeting agents, the impact of sub-inhibitory doses of

compound **22r** on 16S and 23S rRNA expression was assessed by performing real-time qPCR assays using DNA gyrase B (*gyrB*) as reference gene. Relative expression levels of 16S and 23S rRNA in *S. aureus* ATCC® 25923 were probed with SYBR Green system and results were extrapolated using the $\Delta\Delta C_T$ method with each treatment group normalized against the untreated control (Figure 7).

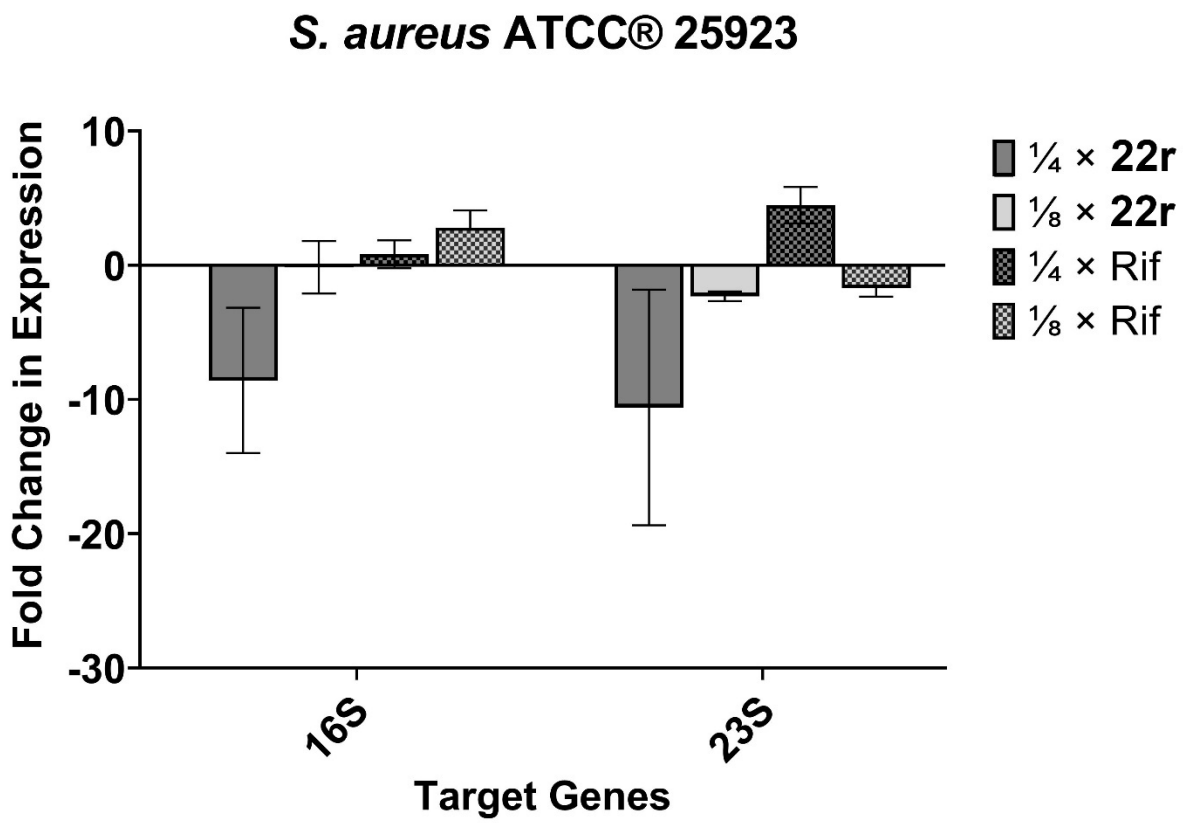

Figure 7. qPCR results on 16S and 23S rRNA expression of *S. aureus* ATCC® 25923 cells treated by rifampicin (Rif) and compound **22r** at different concentrations.

The results showed that both 16S and 23S rRNA expression in *S. aureus* ATCC® 25923 were markedly more downregulated following treatment by ¼ MIC of compound **22r** compared to

all other treatment groups exposed to either lower concentrations of compound **22r** or the positive control drug rifampicin (Figure 7). Trends were indicative of the nusbiarylin compound **22r** appearing to impact rRNA expression by acting upon associated pathways through their purported mechanisms of action, albeit the transcription inhibitor class drug rifampicin not eliciting downregulatory effects at the concentrations used. Given the arrest of staphylococcal growth and resultant degradation in total RNA as shown in Section 3.4, one may take into account that shutdown of bacterial transcription is not permanent due to the maintenance of low levels of ribosomes, and that rifampicin-induced rRNA degradation is both concentration- and time-dependent [34]. When considering mechanistic differences and pathways acted upon by nusbiarylins, it is therefore plausible that the sub-lethal doses of rifampicin employed in our study were insufficient in completely preventing synthesis of new RNA as part of a stress response towards the very presence of rifampicin, where bacteria opt for genetic integrity during subsequent cell divisions as ongoing chromosome replication continues to fruition through DNA synthesis, which is unaffected by transcription inhibition.

3.6 Epifluorescence microscopy

The cellular effects of compound **22r** were examined by fluorescent microscopy as previously described. *B. subtilis* strain BS61 carries a gfp-fused *nusB* gene expressing the green fluorescence protein (GFP)-tagged NusB protein. As expected, fluorescently tagged NusB localized to the central chromosome-containing nucleoid of the cell in the untreated strain (Figure 8 Ctrl). When chloramphenicol was added to the strain, no changes on the localization

of fluorescence can be observed (Figure 8 Chl). In the contrast, rifampicin bound to RNA polymerase and interrupted the transcription function, which can be observed as the delocalization of fluorescence from nucleoid to the whole cell (Figure 8 Rif). **22r** showed antimicrobial activity against *B. subtilis* BS61 with a MIC of 8 μg/mL. When **22r** was added at ⅛ MIC, fluorescence started to delocalize from the nucleoid compared to the untreated control, as the result of decondensed chromosomes at the sub-MIC levels (Figure 8 ⅛ MIC). As the concentration of **22r** increased, diffusion of the fluorescent signal into the cytosol became more significant (Figure 8 ¼ MIC and 1 MIC). These results indicate that **22r** can affect the localization of bacterial transcription complexes at the cellular level.

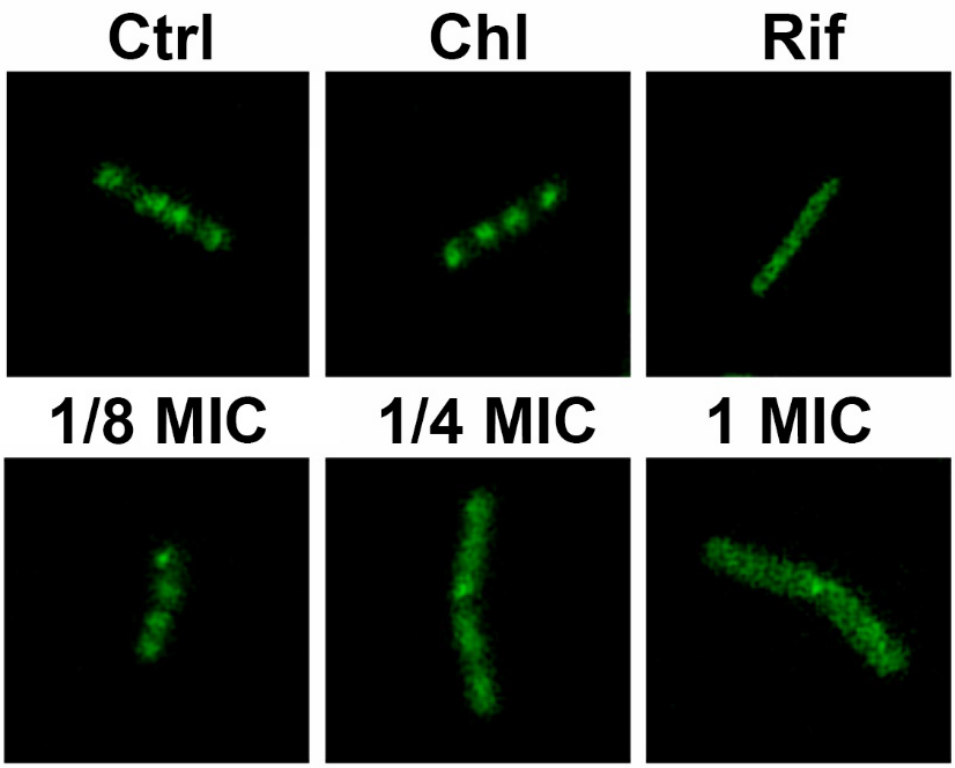

Figure 8. Epifluorescence microscope of *B. subtilis* with NusB fluorescence under treatment of Ctrl (no antibiotics), Chl (chloramphenicol), Rif (rifampicin), and compound **22r** at ⅛, ¼, and 1 MIC.

3.7 Inhibition of NusB-NusE interaction

The inhibitory activity of selected compounds **22e**, **22i**, **22m**, **22o**, and **22r** was measured using an in-house developed protein complement assay [14, 15, 50]. In this assay, NusB and NusE were respectively fused to two complementation fragments of the Nano-Luc luciferase. When a specific inhibitor of the NusB-NusE PPI was added to the reaction, the efficient reformation of the natural luciferase was then reduced. The inhibitory activity of a given compound can be measured by the changes of luminescence, which is due to the inhibition of complemented luciferase catalyzed reaction. As shown in Figure 9, all the selected compounds demonstrated inhibitory activity against the NusB-NusE PPI, in which **22i** and **22r** displayed superior activity to the other tested compounds. Indeed, **22r** also demonstrated the greatest antimicrobial activity. This suggested the antimicrobial activity of the nusbiarylin compounds could be resulted from specific inhibition of NusB-NusE PPI. Although the PPI inhibitory activity did not show a clear correlation to the antimicrobial activity, this phenomenom has been observed in our previous reports [14, 15]. We need to bear in mind that the *in vitro* protein complementation assay was designed to unveal the mechanism of the nusbiarylins, while in real life senarios the antimicrobial activity is related to diverse factors such as the membrane permeability, digestive enzymes, efflux efficiency. Additionally, due to the limitations in the detection range, the *in vitro* assay conditions required high concentrations of the target proteins and nusbiarylin compounds, which may precipitate in the assay and affect the inhibitory activity measurement.

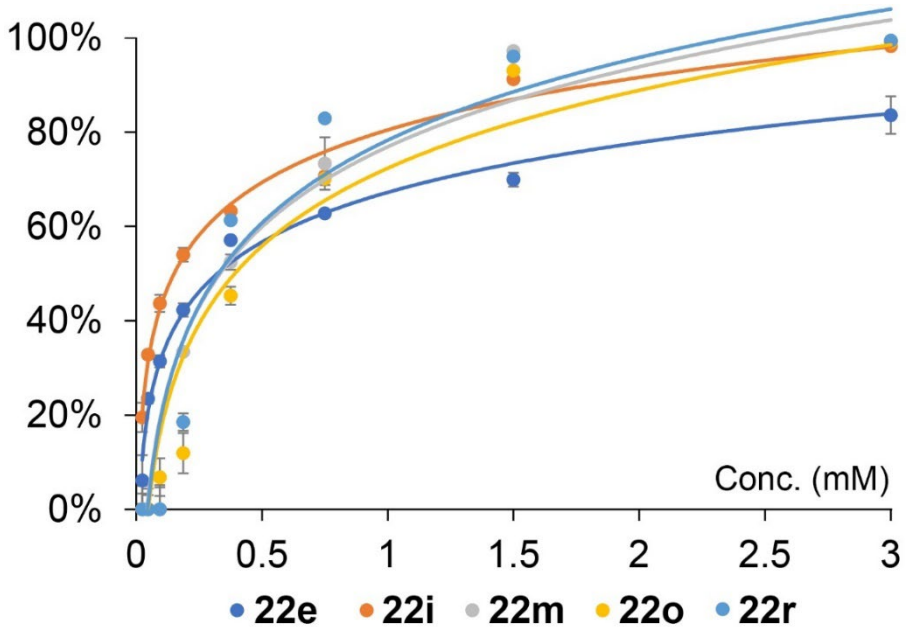

Figure 9. Inhibitory curves of compounds **22e**, **22i**, **22m**, **22o**, and **22r** measured by protein complement assay.

Table 4. IC_{50} values (μM) of compounds **22e**, **22i**, **22m**, **22o**, and **22r**.

	22e	**22i**	**22m**	**22o**	**22r**
IC_{50}	322 ± 13.7	150 ± 7.17	327 ± 48.8	385 ± 60.7	159 ± 10. 6

3.8 *In vitro* cytotoxicity

Four hydrophilic and hydrophobic substituents contained compounds exhibiting antimicrobial activities against *S. aureus* ATCC 25923 were chosen for *in vitro* cytotoxicity testing against human lung carcinoma cell line A549 and human keratinocytes HaCaT. Their cytotoxicity was shown as CC_{50} in Table 5. Apparent therapeutic index (TI) were also calculated to indicate the difference between cytotoxicity and antibacterial activity. Higher the TI value, the more effective and safer a drug would be expected in the future *in vivo* experiment. As shown in the

table, compounds **21h** and **21m** with imine as the linker did not demonstrate significant cytotoxicity towards both A549 and HaCaT, as expected based on previous data [14, 15]. With respect to the cytotoxicity of amine-linked derivatives **22o** and **22r**, their values were also acceptable and showed room for improvement.

Table 5. Cytotoxicity of representative compounds against A549 and HaCaT.

No.	MIC[a] (μg/mL)	CC_{50} (μM)		Therapeutic Index[b]	
		A549	HaCaT	A549	HaCaT
21h	4	81.76 ± 9.65	302.34 ± 16.08	14	52
21m	4	89.67 ± 7.72	>512	15	>89
22o	1	9.38 ± 1.06	16.68 ± 2.61	6	11
22r	0.5	8.89 ± 0.87	5.01 ± 0.25	12	7
DDP[c]	-	7.70 ± 0.58	7.83 ± 0.66	-	-

[a] MIC values against *S. aureus* ATCC 25923.

[b] Calculated by CC_{50} (μM) / ½ MIC (μM)

[c] DDP: cisplatin

3.9 Docking studies

Among the synthesized derivatives, compound **22r** displayed the best antibacterial potency, which was thereby subjected to docking studies to understand the binding mode and guide further optimization.

As indicated from Figure 9, compound **22r** fell into the same binding site as **MC4-2** in a similar bound conformation, where the 5'-NO_2 of compound **22r** formed a hydrogen bond with Tyr18 of NusB and 2'-OH of compound **22r** interacted with Glu81 of NusB, underlying the pivotal

roles of these two groups in the interaction with the hot-spot residues of NusB [14, 15]. Additionally, Figure 10A demonstrated that the 2-phenylethynyl of compound **22r** extended into a small hydrophobic pocket of NusB as expected, implying appropriate hydrophobic substituents at 2-position may promote improved affinity of compound with NusB. Apart from the several amino acid residues that were also involved in the interaction with **MC4-2**, compound **22r** may bind to two additional residues Ala116 and Val80 through hydrophobic interactions, as shown by Figure 10B.

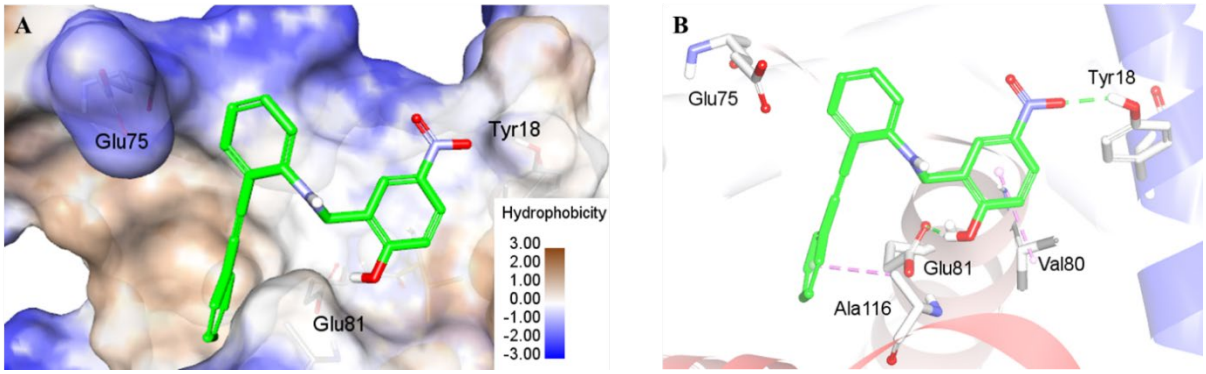

Figure 10. Predicted binding mode of compound **22r** with *E. coli* NusB (PDB: 3D3B). (A) Binding of NusB to compound **22r** (green) with the surface colored by hydrophobicity. (B) Molecular interactions of **22r** with the amino acid residues of NusB: hydrogen bonding interactions (green) and hydrophobic interactions (pink).

3.10 *In silico* drug-like property evaluation

Previously, we evaluated some nusbiarylin compounds and concluded that these compounds possess excellent Caco-2 cell permeability and low hemolytic toxicity [14, 15]. In this study, the three compounds **22o**，**22q** and **22r** with excellent antimicrobial activity were subjected to *in silico* drug-like property evaluation using Schrödinger Maestro 10.2 [35, 36]. Octanol/water

partitioning coefficient (QPlogPo/w), aqueous solubility (QPlogS), binding to human serum albumin (QPlogKhsa), number of likely metabolic reactions (#metab), brain/blood partition coefficient (QPlogBB), apparent MDCK cell permeability (QPPMDCK), central nervous system activity (CNS), apparent Caco-2 cell permeability (QPPCaco), human oral absorption, and predicted IC50 value for blockage of HERG K+ channels (QPlogHERG) were calculated. (Table 6).

Table 6. *In silico* drug-like property evaluation of compounds **22o**, **22q**, and **22r**

Principal descriptors	**22o**	**22q**	**22r**	**Standard Range[a]**
QPlogPo/w	3.932	3.917	4.509	-2.0~6.5
QPlogS	-5.166	-5.277	-5.228	-6.5~0.5
QPlogKhsa	0.574	0.566	0.679	-1.5~1.5
#metab	6	5	6	1~8
QPlogBB	-1.264	-1.338	-1.047	-3.0~1.2
CNS	-2	-2	-2	-2 (inactivity), +2 (activity)
QPPMDCK	180.776	164.354	325.568	< 25 poor, > 500 great
QPPCaco	394.01	360.778	679.03	< 25 poor, > 500 great
(%) Human Oral Absorption	96.424	95.652	100	< 25% is poor, > 80% is high
QPlogHERG	-6.431	-6.687	-6.538	< -5

[a] Statistics of 95% of known drugs by Qikprop (Maestro 10.2).

As shown in Table 6, similar to typic antibiotics, all the 3 selected compounds exhibited the

predicted lipophilicity and aqueous solubility within standard drug-like ranges according to QPlogPo/w and QPlogS values. These results correlate to the multiple phenyl constituents of the molecules. Meanwhile, the compound structures are suggested to be drug-like as the binding to human serum albumin (QPlogKhsa) and the number of likely metabolic reactions (#metab) remained within the standard ranges. The brain/blood partition coefficient (QPlogBB) and the apparent MDCK cell permeability (QPPMDCK) of compounds was predicted to be standard, while the CNS activity was low. The data indicated the compounds could efficiently cross blood-brain barrier through passive diffusion but no CNS activity. It was suggested that the selected compounds possessed good to excellent apparent Caco-2 cell permeability (QPPCaco), which correlated to our previous experiments [14, 15] and implied good oral absorption. Finally, the predicted IC_{50} value for blockage of HERG K+ channels (QPlogHERG) showed that the possiblity of cardiac toxicity was low.

3.11 SAR discussion

With the newly synthesized compounds and antimicrobial activity against *S. aureus* in hand, we concluded the updated SAR which may assist further structural modifications (Figure 11).

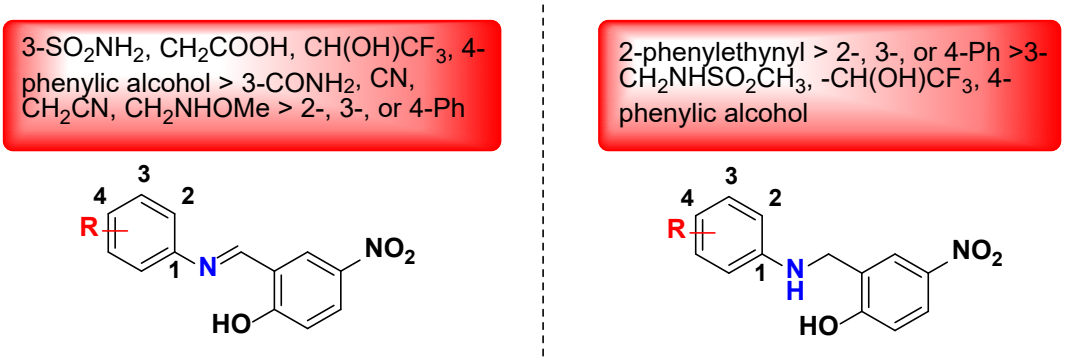

Figure 11. Updated SAR of nusbiarylin compounds

In general, diarylimine derivatives possess good antimicrobial activity regardless the physicochemical properties (2-8 μg/mL), however, hydrogen bonding donors substituted on the left benzene ring may slightly increase the antimicrobial activity (2-4 μg/mL). In the contrast, diarylamine compounds demonstrated diverse antimicrobial activity: compounds with hydrogen bonding donors on the left benzene ring may have mild or lack antimicrobial activity (>64 μg/mL) except **22h**, **22i** and **22m** (8-16 μg/mL), whereas hydrophobic substituents provided excellent antimicrobial activity (0.5-1 μg/mL).

4. Conclusions

Bacterial transcription is a validated but underutilized target for antimicrobial agent discovery [1]. It has been used for antimicrobial agent discovery with diverse structures such as antisense peptide nucleic acid [37], peptides [38], and small molecules [39-46]. Our group previously studied the biological mechanism of bacterial transcription and identified several PPIs important for bacterial cell viability and potential for antimicrobial agent discovery [47-49]. Through targeting the critical binding sites of essential PPIs, we developed the appropriate methods for hit compound identification and derivative screening [50-52] and identified several series of new structures of bacterial transcription inhibitors [53, 54]. Further structural modifications demonstrated the potential of these structures as novel antimicrobial agents [13-15, 17-19]. Nusbiarylins are one of these compounds targeting the PPI of two interacting transcription factors, NusB and NusE. They were named nusbiarylins because of the binding protein NusB and biaryl structure. We found that nusbiarylin structures were very specific with an essential p-nitro phenol responsible for antimicrobial activity, but the other aryl group could

tolerate diverse substitutions and some of them significantly improved antimicrobial activity [14, 15].

In this study, a total of 36 nusbiarylin derivatives were synthesized based on bioisosteric replacement of carboxylic acid and hydrophobic aryl group introduction. These modifications were rationalized according to the previously established SAR in an effort to examine the suitability of different substituents on the left benzene ring. Compounds with the imine linker accepted both hydrophobic and hydrophilic substituents for significant antimicrobial activity, while the amine analogues appeared to be only compatible with hydrophobic groups on the left benzene ring. Some of these compounds, **22o**, **22q**, and **22r**, displayed excellent *in vitro* antimicrobial potency against a wide variety of clinically significant pathogens, including MRSA and VRSA strains, while compound **22r** especially demonstrated superior antimicrobial activity with an MIC of 0.5 μg/mL compared to control antibiotics. The mechanistic studies showed that as a representative nusbiarylin compound, **22r** could inhibit bacterial ATP production as a bacteriostatic agent and reduced the total RNA and protein production of bacteria. However, **22r** specifically inhibited bacterial rRNA synthesis in the contrast to rifampicin as a general transcription inhibitor. Additionally, **22r** interrupted the function of NusB protein similarly to rifampicin, demonstrated by epifluorescence microscopy. Molecular docking study was performed to compare lead compounds **MC4-2**, **MC4-6** and the representative compound **22r** obtained in this study. The docking study showed that both amine **MC4-2** and imine **MC4-6** similarly bound to the same binding site, while **22r** with an additionally ethynyl group protruding the phenyl group to the hydrophobic binding site, which slightly changed the binding pose for additional interactions with Ala116 and Val80 of NusB

protein. As the binding site at NusB belongs to a PPI site, which is relatively flat and more challenging to maintain the same binding pose for small molecule ligands. Nevertheless, the biological evaluations and docking study indicated that the compounds fulfilled the requirement of the pharmacophore model commonly exhibited affinity to the targeted protein NusB and antimicrobial activity, while the physico-chemical properties such as lipophilicity of compounds also affected antimicrobial activity, probably by membrane permeability. In summary, The discovery of **22r** encouraged us to explore more structural diversity of nusbiarylins for new antimicrobial agent discovery.

5. Experimental section

5.1 Chemistry

5.1.1 Materials and chemicals

Starting materials and regents, unless otherwise stated, were of commercial grade and were used without further purification. All reactions were monitored by thin-layer chromatography (TLC) on glass sheets (silica gel F254) which can be visualized under 256 nm UV light. Flash chromatography was carried out using silica-gel (200-300 mesh). ^{1}H NMR (400 MHz) and ^{13}C NMR (100 MHz) spectra were measured on Bruker Avance-III spectrometer with TMS as an internal standard. High-resolution MS spectra were measured using a Micromass® QTOF-2 spectrometer by electron spray ionization [55].

5.1.2 General procedure (A) for synthesis of imine-linked derivatives

To a solution of benzaldehydes (1 equiv) in ethanol (10 mL) was added anilines (1 equiv), and

the reaction mixture was stirred at room temperature overnight. The solid was collected by filtration and washed with ethanol and hexane.

5.1.3 (*E*)-3-((2-hydroxy-5-nitrobenzylidene)amino)benzamide (**21a**)

The title compound was prepared according to general procedure (**A**) using 5-nitrosalicylaldehyde **1** (100 mg, 0.60 mmol) and 3-aminobenzamide **2** (81 mg, 0.60 mmol, 1 equiv), yielding the pure product as a yellow solid (144 mg, 84%). ^{1}H NMR (400 MHz, DMSO-d_6) δ 14.13 (br s, 1H), 9.21 (s, 1H), 8.70 (d, J = 3.0 Hz, 1H), 8.27 (dd, J = 9.2, 2.9 Hz, 1H), 8.09 (s, 1H), 7.98 (s, 1H), 7.86 (d, J = 7.5 Hz, 1H), 7.70 – 7.42 (m, 3H), 7.15 (d, J = 9.2 Hz, 1H); ^{13}C NMR (100 MHz, DMSO-d_6) δ 167.7, 166.9, 162.4, 147.4, 139.8, 136.2, 130.0, 129.0, 128.6, 127.0, 124.6, 121.0, 119.3, 118.7; HRMS (ESI) calcd for $C_{14}H_{10}N_3O_4$ [M-H]$^-$ 284.0677, found 284.0674.

5.1.4 (*E*)-3-((2-hydroxy-5-nitrobenzylidene)amino)benzenesulfonamide (**21b**)

The title compound was prepared according to general procedure (**A)** using 5-nitrosalicylaldehyde **1** (100 mg, 0.60 mmol) and 3-aminobenzenesulfonamide **3** (103 mg, 0.60 mmol, 1 equiv), yielding the pure product as a yellow solid (176 mg, 92%). ^{1}H NMR (400 MHz, DMSO-d_6) δ 13.64 (s, 1H), 9.18 (s, 1H), 8.74 (d, J = 3.0 Hz, 1H), 8.30 (dd, J = 9.2, 3.0 Hz, 1H), 7.87 (s, 1H), 7.85 – 7.74 (m, 1H), 7.74 – 7.64 (m, 2H), 7.47 (s, 2H), 7.18 (d, J = 9.2 Hz, 1H); ^{13}C NMR (100 MHz, DMSO-d_6) δ 166.2, 162.6, 148.6, 145.9, 140.0, 130.8, 129.1, 128.1, 125.2, 124.7, 119.8, 119.1, 118.5, 40.62, 40.4, 40.2, 40.0, 39.8, 39.6, 39.4; HRMS (ESI) calcd for $C_{13}H_{10}N_3O_5S$ [M-H]$^-$ 320.0347, found 320.0347.

5.1.5 (*E*)-2-((2-hydroxy-5-nitrobenzylidene)amino)benzonitrile (**21c**)

The title compound was prepared according to general procedure (**A)** using 5-nitrosalicylaldehyde **1** (100 mg, 0.60 mmol) and 2-aminobenzonitrile **4** (71 mg, 0.60 mmol, 1 equiv), yielding the pure product as a yellow solid (129 mg, 81%). ^{1}H NMR (400 MHz, DMSO-d_6) δ 9.22 (s, 1H), 8.75 (d, J = 2.9 Hz, 1H), 8.32 (dd, J = 9.1, 3.0 Hz, 1H), 7.95 (d, J = 7.7 Hz, 1H), 7.84 (t, J = 7.8 Hz, 1H), 7.69 (d, J = 8.2 Hz, 1H), 7.51 (t, J = 7.6 Hz, 1H), 7.17 (d, J = 9.2 Hz, 1H); ^{13}C NMR (100 MHz, $CDCl_3$) δ 166.5, 163.3, 149.7, 134.1, 133.5, 129.4, 129.0, 128.1, 118.8, 118.5, 117.7, 116.6, 109.1; HRMS (ESI) calcd for $C_{14}H_8N_3O_3$ $[M-H]^-$ 266.0571, found 266.0569.

5.1.6 (*E*)-3-((2-hydroxy-5-nitrobenzylidene)amino)benzonitrile (**21d**)

The title compound was prepared according to general procedure (**A**) using 5-nitrosalicylaldehyde **1** (100 mg, 0.60 mmol) and 3-aminobenzonitrile **5** (71 mg, 0.60 mmol, 1 equiv), yielding the pure product as a yellow solid (129 mg, 81%). ^{1}H NMR (400 MHz, $CDCl_3$) δ 13.62 (s, 1H), 8.75 (s, 1H), 8.46 (d, J = 2.8 Hz, 1H), 8.34 (dd, J = 9.2, 2.7 Hz, 1H), 7.70 – 7.54 (m, 4H), 7.17 (d, J = 9.2 Hz, 1H); ^{13}C NMR (100 MHz, $CDCl_3$) δ 166.3, 163.0, 148.1, 140.4, 131.2, 130.7, 129.1, 128.8, 125.66, 124.9, 118.5, 117.9, 117.8, 114.0; HRMS (ESI) calcd for $C_{14}H_8N_3O_3$ $[M-H]^-$ 266.0571, found 266.0569.

5.1.7 (*E*)-4-((2-hydroxy-5-nitrobenzylidene)amino)benzonitrile (**21e**)

The title compound was prepared according to general procedure (**A)** using 5-

nitrosalicylaldehyde **1** (100 mg, 0.60 mmol) and 4-aminobenzonitrile **6** (71 mg, 0.60 mmol, 1 equiv), yielding the pure product as a yellow solid (133 mg, 83%). ^{1}H NMR (400 MHz, $CDCl_3$) δ 13.62 (s, 1H), 8.74 (s, 1H), 8.46 (d, *J* = 2.8 Hz, 1H), 8.35 (dd, *J* = 9.1, 2.8 Hz, 1H), 7.87 – 7.76 (m, 2H), 7.42 (d, *J* = 8.4 Hz, 2H), 7.17 (d, *J* = 9.2 Hz, 1H); ^{13}C NMR (100 MHz, $CDCl_3$) δ 166.4, 163.3, 150.9, 140.4, 133.8, 129.2, 128.9, 122.1, 118.6, 118.2, 117.8, 111.4; HRMS (ESI) calcd for $C_{14}H_8N_3O_3$ $[M-H]^-$ 266.0571, found 266.0570.

5.1.8 (*E*)-2-(3-((2-hydroxy-5-nitrobenzylidene)amino)phenyl)acetonitrile (**21f**)

The title compound was prepared according to general procedure (**A**) using 5-nitrosalicylaldehyde **1** (100 mg, 0.60 mmol) and 2-(3-aminophenyl)acetonitrile **7** (79 mg, 0.6 mmol, 1 equiv), yielding the pure product as a yellow solid (145 mg, 86%). ^{1}H NMR (400 MHz, $CDCl_3$) δ 14.08 (s, 1H), 8.75 (s, 1H), 8.44 (d, *J* = 2.8 Hz, 1H), 8.31 (dd, *J* = 9.1, 2.8 Hz, 1H), 7.52 (t, *J* = 7.7 Hz, 1H), 7.38 – 7.29 (m, 3H), 7.14 (d, *J* = 9.2 Hz, 1H), 3.86 (s, 2H); ^{13}C NMR (100 MHz, $CDCl_3$) δ 166.6, 161.7, 147.8, 140.1, 131.7, 130.5, 128.6, 128.6, 127.4, 121.1, 120.8, 118.4, 118.0, 117.4, 23.5; HRMS (ESI) calcd for $C_{15}H_{10}N_3O_3$ $[M-H]^-$ 280.0728, found 280.0725.

5.1.9 (*E*)-2-(3-((2-hydroxy-5-nitrobenzylidene)amino)phenyl)acetic acid (**21g**)

The title compound was prepared according to general procedure (**A)** using 5-nitrosalicylaldehyde **1** (100 mg, 0.60 mmol) and 3-aminophenylacetic acid **8** (90 mg, 0.60 mmol, 1 equiv), yielding the pure product as a yellow solid (153 mg, 85%). ^{1}H NMR (400 MHz, DMSO-d_6) δ 14.42 (br s, 1H), 12.43 (br s, 1H), 9.20 (s, 1H), 8.70 (d, *J* = 2.9 Hz, 1H),

8.28 (dd, J = 9.1, 3.0 Hz, 1H), 7.52 – 7.34 (m, 3H), 7.28 (d, J = 7.4 Hz, 1H), 7.13 (d, J = 9.1 Hz, 1H), 3.67 (s, 2H); ^{13}C NMR (100 MHz, DMSO-d_6) δ 172.9, 167.6, 162.0, 146.8, 139.5, 137.1, 129.9, 129.3, 128.9, 128.9, 123.2, 119.9, 119.0, 118.9, 40.9; HRMS (ESI) calcd for $C_{15}H_{11}N_2O_5$ $[M-H]^-$ 299.0673, found 299.0677.

5.1.10 (*E*)-*N*-(3-((2-hydroxy-5-nitrobenzylidene)amino)benzyl)methanesulfonamide (**21h**)

Step 1: *N*-(3-nitrobenzyl)methanesulfonamide (**24**). To a mixture of 3-nitrobenzaldehyde **23** (500 mg, 3.31 mmol) and methanesulfonamide (472 mg, 4.96 mmol, 1.5 equiv) in toluene (10 mL) was added titanium(IV) ethoxide (2130 μL, 6.62 mmol, 2 equiv). The resulting mixture was stirred at 110℃ for 4 h. Upon completion, the reaction mixture was concentrated under reduced pressure. The residue was redissolved in a mixture of THF/MeOH (10 mL, 1:1, v/v), followed by the addition of sodium borohydride (626 mg, 16.54 mmol, 5 equiv). The resulting mixture was stirred at room temperature for 3 h. Upon completion, the reaction mixture was extracted with ethyl acetate (EA) (20 mL × 3). The organic layers were combined, washed with brine, dried over Na_2SO_4, filtered, and concentrated under reduced pressure. The pure product was obtained as a yellow solid (525 mg, 69%) by flash chromatography (Hexane:EA = 5:1, v/v). ^{1}H NMR (400 MHz, DMSO-d_6) δ 8.24 (t, J = 2.0 Hz, 1H), 8.15 (ddd, J = 1.0, 2.4, 8.3 Hz, 1H), 7.81 (dt, J = 1.3, 7.7 Hz, 1H), 7.76 (t, J = 6.4 Hz, 1H), 7.67 (t, J = 7.9 Hz, 1H), 4.32 (d, J = 6.4 Hz, 2H), 2.94 (s, 3H).

Step 2: *N*-(3-aminobenzyl)methanesulfonamide (**9**). To a solution of **24** (525 mg, 2.28 mmol) in a mixture of EtOH/water (14 mL, 5:2, v/v) was added NH_4Cl (610 mg, 11.40 mmol, 5 equiv) and iron powder (637 mg, 5.97 mmol, 5 equiv). The resulting mixture was stirred at 80℃ for

1 h. Upon completion, the reaction mixture was filtered through a short pad of Celite and the filtrate was extracted with EA (20 mL × 3). The organic layers were combined, washed with brine, dried over Na_2SO_4, filtered, concentrated under reduced pressure, and dried *in vacuo* to afford the crude product **9** as a yellow solid (370 mg, 81%), which was used directly in the next step without further purification.

Step 3: The title compound was prepared according to general procedure (**A)** using 5-nitrosalicylaldehyde **1** (83 mg, 0.50 mmol) and **9** (100 mg, 0.50 mmol, 1 equiv), yielding the pure product as a yellow solid (143 mg, 82%). ^{1}H NMR (400 MHz, DMSO-d_6) δ 14.34 (br s, 1H), 9.19 (s, 1H), 8.71 (d, J = 2.9 Hz, 1H), 8.28 (dd, J = 2.9, 9.2 Hz, 1H), 7.63 (t, J = 6.4 Hz, 1H), 7.50 (t, J = 7.7 Hz, 1H), 7.45 (d, J = 1.9 Hz, 1H), 7.45 – 7.37 (m, 1H), 7.39 – 7.32 (m, 1H), 7.14 (d, J = 9.1 Hz, 1H), 4.24 (d, J = 6.3 Hz, 2H), 2.91 (s, 3H); ^{13}C NMR (100 MHz, DMSO-d_6) δ 167.4, 161.9, 147.1, 140.5, 139.5, 130.1, 128.9, 128.8, 127.4, 121.3, 120.4, 119.1, 118.8, 46.2; HRMS (ESI) calcd for $C_{15}H_{14}N_3O_5S$ $[M-H]^-$ 348.0660, found 348.0662.

5.1.11 (*E*)-4-nitro-2-(((3-(2,2,2-trifluoro-1-hydroxyethyl)phenyl)imino)methyl)phenol (**21i**)

Step 1: 2,2,2-trifluoro-1-(3-nitrophenyl)ethan-1-one (**26**). To a solution of 2,2,2-trifluoro-1-phenylethan-1-one **25** (100 mg, 0.57 mmol) in concentrated sulfuric acid (2 mL) was added potassium nitrate (75 mg, 0.75 mmol, 1.3 equiv) at 0°C. The resulting mixture was stirred at the same temperature for 10 min. Upon completion, the reaction mixture was added ice-cold water. The formed precipitate was filtered, collected, and dried *in vacuo* to afford the crude product as a yellow solid (93 mg, 74%), which was used directly in the next step without further purification.

Step 2: 1-(3-aminophenyl)-2,2,2-trifluoroethan-1-ol (**10**). To a solution of **26** (93 mg, 0.42 mmol) in EtOH (5 mL) was added sodium borohydride (16 mg, 0.42 mmol, 1 equiv). The resulting mixture was stirred at room temperature for 1 h. Upon completion, the reaction mixture was concentrated under reduced pressure. The residue was redissolved in a mixture of EtOH/water (7 mL, 5:2, v/v), followed by the addition of NH_4Cl (114 mg, 2.12 mmol, 5 equiv) and iron powder (119 mg, 2.12 mmol, 5 equiv). The resulting mixture was stirred at 80℃ for 1 h. Upon completion, the reaction mixture was filtered through a short pad of Celite and the filtrate was extracted with EA (10 mL × 3). The organic layers were combined, washed with brine, dried over Na_2SO_4, filtered, and concentrated under reduced pressure. The pure product was obtained as a colorless oil (68 mg, 84%) by flash chromatography (Hexane:EA = 5:1, v/v). ^{1}H NMR (400 MHz, $CDCl_3$) δ 7.20 (t, *J* = 7.8 Hz, 1H), 6.86 (d, *J* = 7.6 Hz, 1H), 6.80 (s, 1H), 6.73 (dd, *J* = 2.3, 8.1 Hz, 1H), 4.92 (q, *J* = 6.8 Hz, 1H), 3.76 (s, 2H), 2.84 (s, 1H).

Step 3: The title compound was prepared according to general procedure (**A)** using 5-nitrosalicylaldehyde **1** (59 mg, 0.35 mmol) and **10** (68 mg, 0.35 mmol, 1 equiv), yielding the pure product as a yellow solid (99 mg, 82%). ^{1}H NMR (400 MHz, $CDCl_3$) δ 14.19 (s, 1H), 8.76 (s, 1H), 8.44 (d, *J* = 2.7 Hz, 1H), 8.31 (dd, *J* = 9.1, 2.8 Hz, 1H), 7.55 (t, *J* = 7.7 Hz, 1H), 7.52 – 7.45 (m, 2H), 7.40 (dt, *J* = 7.8, 1.9 Hz, 1H), 7.14 (d, *J* = 9.1 Hz, 1H), 5.15 (q, *J* = 6.6 Hz, 1H), 2.78 (s, 1H); ^{13}C NMR (100 MHz, DMSO-d_6) δ 167.0, 162.2, 147.2, 139.7, 138.0, 130.0, 128.9, 128.8, 127.3, 125.4 (d, *J* = 282.8 Hz), 122.1, 121.3, 119.3, 118.7, 70.6 (q, *J* = 30.4 Hz); HRMS (ESI) calcd for $C_{15}H_{10}F_3N_2O_4$ $[M-H]^-$ 339.0598, found 339.0601.

5.1.12 (*E*)-3-((2-hydroxy-5-nitrobenzylidene)amino)-N-methoxybenzamide (**21j**)

Step 1: 3-((*tert*-butoxycarbonyl)amino)benzoic acid (**28**). To a solution of 3-aminobenzoic acid **27** (200 mg, 1.46 mmol) in a mixture of dioxane/water (1:1, v/v, 4 mL) was added $(Boc)_2O$ (414 mg, 1.90 mmol, 1.3 equiv) in dixoane (2 mL) and triethylamine (TEA) (304 μL, 2.19 mmol, 1.5 equiv). The resulting mixture was stirred at room temperature for 4 h. Upon completion, the reaction mixture was concentrated under reduced pressure, washed with hexane, and dried *in vacuo* to afford the crude product as a white solid (313 mg, 90%), which was used directly in the next step without further purification.

Step 2: *tert*-butyl (3-(methoxycarbamoyl)phenyl)carbamate (**29**). To a solution of **28** (100 mg, 0.42 mmol) in anhydrous dichloromethane (DCM) (5 mL) was added EDC·HCl (162 mg, 0.84 mmol, 2 equiv), 4-dimethylaminopyridine (DMAP) (51 mg, 0.42 mmol, 1 equiv), *N*,*N*-diisopropylethylamine (DIEA) (250 μL, 1.52 mmol, 3.6 equiv) and methoxyammonium chloride (46 mg, 0.55 mmol, 1.3 equiv). The resulting mixture was stirred at room temperature overnight. Upon completion, the reaction mixture was extracted with EA (10 mL × 3). The organic layers were combined, washed with 1N hydrochloride acid and brine, dried over Na_2SO_4, filtered, concentrated under reduced pressure and dried *in vacuo* to afford the crude product as a white solid (75 mg, 67%), which was used directly in the next step without further purification.

Step 3: 3-amino-*N*-methoxybenzamide (**11**). To a solution of **29** (75 mg, 0.28 mmol) in anhydrous DCM (6 mL) was added TFA (1 mL). The resulting mixture was stirred at room temperature for 3 h. Upon completion, the reaction mixture was concentrated under reduced pressure and dried *in vacuo* to afford the crude product as a grey solid (43 mg, 92%), which was used directly in the next step without further purification.

Step 4: The title compound was prepared according to general procedure (**A**) using **29** (43 mg, 0.26 mmol) and 5-nitrosalicylaldehyde **1** (43 mg, 0.26 mmol, 1 equiv), yielding the pure product as a yellow solid (63 mg, 78%). ^{1}H NMR (400 MHz, DMSO-d_6) δ 13.97 (br s, 1H), 11.87 (s, 1H), 9.20 (s, 1H), 8.70 (d, J = 2.9 Hz, 1H), 8.28 (dd, J = 9.2, 3.0 Hz, 1H), 7.83 (s, 1H), 7.73 (d, J = 7.5 Hz, 1H), 7.65 (d, J = 8.0 Hz, 1H), 7.59 (t, J = 7.7 Hz, 1H), 7.15 (d, J = 9.1 Hz, 1H), 3.74 (s, 3H); ^{13}C NMR (100 MHz, DMSO-d_6) δ 166.6, 163.8, 162.5, 147.7, 139.9, 134.1, 130.3, 129.0, 128.5, 126.5, 125.0, 120.6, 119.4, 118.6, 63.8; HRMS (ESI) calcd for $C_{15}H_{12}N_3O_5$ $[M-H]^-$ 314.0782, found 314.0780.

5.1.13 (*E*)-3-((2-hydroxy-5-nitrobenzylidene)amino)-*N*-(methylsulfonyl)benzamide (**21k**)

Step 1: *tert*-butyl (3-((methylsulfonyl)carbamoyl)phenyl)carbamate (**30**). To a solution of **28** (100 mg, 0.42 mmol) in anhydrous DCM (5 mL) was added EDC·HCl (162 mg, 0.84 mmol, 2 equiv), DMAP (51 mg, 0.42 mmol, 1 equiv), DIEA (174 μL, 1.05 mmol, 2.5 equiv) and methanesulfonamide (52 mg, 0.55 mmol, 1.3 equiv). The resulting mixture was stirred at room temperature overnight. Upon completion, the reaction mixture was extracted with EA (10 mL × 3). The organic layers were combined, washed with 1N hydrochloride acid and brine, dried over Na_2SO_4, filtered, concentrated under reduced pressure and dried *in vacuo* to afford the crude product as a white solid (97 mg, 73%), which was used directly in the next step without further purification.

Step 2: 3-amino-*N*-(methylsulfonyl)benzamide (**12**). To a solution of **30** (97 mg, 0.31 mmol) in anhydrous DCM (6 mL) was added TFA (1 mL). The resulting mixture was stirred at room temperature for 3 h. Upon completion, the reaction mixture was concentrated under reduced

pressure and dried *in vacuo* to afford the crude product as a grey solid (58 mg, 88%), which was used directly in the next step without further purification.

Step 3: The title compound was prepared according to general procedure (**A**) using **12** (58 mg, 0.27 mmol) and 5-nitrosalicylaldehyde **1** (45 mg, 0.27 mmol, 1 equiv), yielding the pure product as a yellow solid (91 mg, 93%). ^{1}H NMR (400 MHz, DMSO-d_6) δ 13.83 (br s, 1H), 11.76 (br s, 1H), 9.21 (s, 1H), 8.70 (d, J = 3.0 Hz, 1H), 8.29 (dd, J = 9.2, 2.9 Hz, 1H), 8.05 (s, 1H), 7.91 (d, J = 7.7 Hz, 1H), 7.75 (d, J = 7.0 Hz, 1H), 7.65 (t, J = 7.8 Hz, 1H), 7.17 (d, J = 9.1 Hz, 1H), 3.41 (s, 3H); ^{13}C NMR (100 MHz, DMSO-d_6) δ 166.5, 166.3, 162.6, 147.9, 140.0, 133.5, 130.4, 129.0, 128.4, 127.8, 126.7, 121.8, 119.5, 118.6, 41.8; HRMS (ESI) calcd for $C_{15}H_{12}N_3O_6S$ $[M-H]^-$ 362.0452, found 362.0449.

5.1.14 (*E*)-*N*-(*N*,*N*-dimethylsulfamoyl)-3-((2-hydroxy-5-nitrobenzylidene)amino)benzamide (**21l**)

Step 1: *tert*-butyl (3-((*N*,*N*-dimethylsulfamoyl)carbamoyl)phenyl)carbamate (**31**). To a solution of **28** (100 mg, 0.42 mmol) in anhydrous DCM (5 mL) was added 1-ethyl-3-(3-dimethylaminopropyl)carbodiimide (EDC)·HCl (162 mg, 0.84 mmol, 2 equiv), DMAP (51 mg, 0.42 mmol, 1 equiv), DIEA (174 μL, 1.05 mmol, 2.5 equiv) and *N*,*N*-dimethylsulfamide (68 mg, 0.55 mmol, 1.3 equiv). The resulting mixture was stirred at room temperature overnight. Upon completion, the reaction mixture was extracted with EA (10 mL × 3). The organic layers were combined, washed with 1N hydrochloride acid and brine, dried over Na_2SO_4, filtered, concentrated under reduced pressure and dried *in vacuo* to afford the crude product as a white solid (105 mg, 73%), which was used directly in the next step without further purification.

Step 2: 3-amino-*N*-(*N*,*N*-dimethylsulfamoyl)benzamide (**13**). To a solution of **31** (105 mg, 0.31 mmol) in anhydrous DCM (6 mL) was added TFA (1 mL). The resulting mixture was stirred at room temperature for 3 h. Upon completion, the reaction mixture was concentrated under reduced pressure and dried *in vacuo* to afford the crude product as a grey solid (63 mg, 85%), which was used directly in the next step without further purification.

Step 3: The title compound was prepared according to general procedure (**A**) using **13** (63 mg, 0.26 mmol) and 5-nitrosalicylaldehyde **1** (43 mg, 0.26 mmol, 1 equiv), yielding the pure product as a yellow solid (87 mg, 86%). ^{1}H NMR (400 MHz, DMSO-d_6) δ 13.91 (br s, 1H), 11.93 (br s, 1H), 9.22 (s, 1H), 8.71 (d, J = 3.0 Hz, 1H), 8.29 (dd, J = 9.1, 3.0 Hz, 1H), 8.04 (s, 1H), 7.90 (d, J = 7.9 Hz, 1H), 7.74 (d, J = 8.1 Hz, 1H), 7.64 (t, J = 7.8 Hz, 1H), 7.23 – 7.11 (m, 1H), 2.92 (s, 6H); ^{13}C NMR (100 MHz, DMSO-d_6) δ 166.5, 165.7, 162.6, 147.8, 140.0, 133.6, 130.3, 129.0, 128.4, 127.7, 126.4, 121.68, 119.5, 118.6, 38.4; HRMS (ESI) calcd for $C_{16}H_{15}N_4O_6S$ $[M-H]^-$ 391.0718, found 391.0712.

5.1.15 (*E*)-3-(3-((2-hydroxy-5-nitrobenzylidene)amino)phenyl)-1,2,4-oxadiazol-5(4*H*)-one (**21m**)

Step 1: *tert*-butyl (3-cyanophenyl)carbamate (**32**). To a solution of 3-aminobenzonitrile **5** (500 mg, 4.23 mmol) in EtOH (10 mL) was added $(Boc)_2O$ (1016 mg, 4.66 mmol, 1.1 equiv). The resulting mixture was stirred at room temperature overnight. Upon completion, the reaction mixture was concentrated under reduced pressure, washed with hexane, and dried *in vacuo* to afford the crude product as a white solid (804 mg, 87%), which was used directly in the next step without further purification.

Step 2: *tert*-butyl (3-(5-oxo-4,5-dihydro-1,2,4-oxadiazol-3-yl)phenyl)carbamate (**33**). To a solution of **32** (100 mg, 0.46 mmol) in EtOH (5 mL) was added TEA (160 μL, 1.15 mmol, 2.5 equiv) and hydroxylamine hydrochloride (80 mg, 1.15 mmol, 2.5 equiv). The resulting mixture was stirred at 80℃ for 3 h. Upon completion, the reaction mixture was extracted with EA (10 mL × 3). The organic layers were combined, washed with brine, dried over Na_2SO_4, filtered, and concentrated under reduced pressure. The residue was redissolved in THF (10 mL), followed by the addition of pyridine (41 μL, 0.50 mmol, 1.1 equiv) and 2-ethylhexyl chloroformate (50 μL, 0.50 moml, 1.1 equiv) at 0℃. The resulting mixture was stirred at the same temperature for 30 min before being concentrated under reduced pressure. The residue was redissolved in xylene (10 mL) and stirred at 140℃ for 3 h. Upon completion, the reaction mixture was extracted with EA (10 mL × 3). The organic layers were combined, washed with brine, dried over Na_2SO_4, filtered, and concentrated under reduced pressure. The pure product was obtained as a white solid (62 mg, 49%) by flash chromatography (Hexane:EA = 3:1, v/v). ^{1}H NMR (400 MHz, DMSO-d_6) δ 12.96 (s, 1H), 9.66 (s, 1H), 8.08 (s, 1H), 7.58 (dt, J = 1.5, 8.2 Hz, 1H), 7.46 (t, J = 7.9 Hz, 1H), 7.37 (dt, J = 1.3, 7.8 Hz, 1H), 1.49 (s, 9H).

Step 3: 3-(3-aminophenyl)-1,2,4-oxadiazol-5(4*H*)-one (**14**). To a solution of **33** (53 mg, 0.19 mmol) in anhydrous DCM (6 mL) was added TFA (1 mL). The resulting mixture was stirred at room temperature for 3 h. Upon completion, the reaction mixture was concentrated under reduced pressure and dried *in vacuo* to afford the crude product as a grey solid (30 mg, 88%), which was used directly in the next step without further purification.

Step 4: The title compound was prepared according to general procedure (**A)** using 5-nitrosalicylaldehyde **1** (28 mg, 0.17 mmol) and **14** (30 mg, 0.17 mmol, 1 equiv), yielding the

pure product as a yellow solid (51 mg, 94%). ^{1}H NMR (400 MHz, Acetone-d_6) δ 14.14 (br s, 1H), 11.62 (br s, 1H), 9.28 (s, 1H), 8.67 (d, J = 2.8 Hz, 1H), 8.36 (dd, J = 2.8, 9.3 Hz, 1H), 8.03 (s, 1H), 7.90 (d, J = 7.6 Hz, 1H), 7.82 (d, J = 8.0 Hz, 1H), 7.76 (t, J = 7.8 Hz, 1H), 7.21 (d, J = 9.3 Hz, 1H); ^{13}C NMR (100 MHz, DMSO-d_6) δ 166.4, 162.4, 160.8, 157.8, 148.7, 139.9, 131.0, 129.0, 128.1, 125.2, 125.2, 119.7, 119.7, 118.5; HRMS (ESI) calcd for $C_{15}H_9N_4O_5$ [M-H]$^-$ 325.0578, found 325.0578.

5.1.16 (*E*)-3,5-difluoro-3'-((2-hydroxy-5-nitrobenzylidene)amino)-[1,1'-biphenyl]-4-ol (**21n**)

Step 1: 2-(allyloxy)-5-bromo-1,3-difluorobenzene (**35**). To a mixture of 4-bromo-2,6-difluorophenol **34** (500 mg, 2.39 mmol) in acetone (20 mL) was added allyl bromide (250 μL, 2.87 mmol, 1.2 equiv) and potassium carbonate (430 mg, 3.11 mmol, 1.3 equiv). The resulting mixture was stirred at 60°C for 3 h. Upon completion, the reaction mixture was extracted with DCM (10 mL × 3). The organic layers were combined, washed with brine, dried over Na_2SO_4, filtered, concentrated under reduced pressure, and dried *in vacuo* to afford the crude product as a colorless oil (387 mg, 65%), which was used directly in the next step without further purification.

Step 2: 3,5-difluoro-3'-nitro-[1,1'-biphenyl]-4-ol (**37**). To a mixture of **35** (600 mg, 2.41 mmol), 3-nitrophenylboronic acid **36** (483 mg, 2.89 mmol, 1.2 equiv), $Pd(PPh_3)_4$ (84 mg, 0.07 mmol, 0.03 equiv) and tripotassium phosphate (1023 mg, 4.82 mmol, 2 equiv) was added a mixture of dimethoxyethane/water (10 mL, 4:1, v/v) under N_2 atmosphere. The resulting mixture was stirred at 100°C for 18 h. Upon completion, the reaction mixture was extracted with EA (10 mL × 3). The organic layers were combined, washed with brine, dried over Na_2SO_4, filtered,

and concentrated under reduced pressure. The pure product was obtained as a white solid (430 mg, 71%) by flash chromatography (Hexane:EA = 20:1, v/v). ^{1}H NMR (400 MHz, $CDCl_3$) δ 8.39 (t, *J* = 2.1 Hz, 1H), 8.24 (ddd, *J* = 1.1, 2.3, 8.2 Hz, 1H), 7.85 (dt, *J* = 1.5, 7.6 Hz, 1H), 7.64 (t, *J* = 8.0 Hz, 1H), 7.26 – 7.19 (m, 2H), 5.28 (s, 1H).

Step 3: 3'-amino-3,5-difluoro-[1,1'-biphenyl]-4-ol (**15**). To a solution of **37** (300 mg, 1.19 mmol) in a mixture of EtOH/water (14 mL, 5:2, v/v) was added NH_4Cl (319 mg, 5.97 mmol, 5 equiv) and iron powder (334 mg, 5.97 mmol, 5 equiv). The resulting mixture was stirred at 80℃ for 1 h. Upon completion, the reaction mixture was filtered through a short pad of Celite and the filtrate was extracted with EA (10 mL × 3). The organic layers were combined, washed with brine, dried over Na_2SO_4, filtered, concentrated under reduced pressure, and dried *in vacuo* to afford the crude product as a colorless oil (227 mg, 86%), which was used directly in the next step without further purification.

Step 4: The title compound was prepared according to general procedure (**A)** using 5-nitrosalicylaldehyde **1** (76 mg, 0.45 mmol) and **15** (100 mg, 0.45 mmol, 1 equiv), yielding the pure product as a yellow solid (156 mg, 93%). ^{1}H NMR (400 MHz, DMSO-d_6) δ 14.38 (s, 1H), 10.40 (s, 1H), 9.30 (s, 1H), 8.69 (d, *J* = 2.9 Hz, 1H), 8.29 (dd, *J* = 9.2, 2.9 Hz, 1H), 7.85 (t, *J* = 2.0 Hz, 1H), 7.69 (dt, *J* = 7.9, 1.2 Hz, 1H), 7.61 – 7.49 (m, 3H), 7.46 (dd, *J* = 7.6, 2.0 Hz, 1H), 7.15 (d, *J* = 9.3 Hz, 1H); ^{13}C NMR (100 MHz, DMSO-d_6) δ 167.74, 162.53, 153.11 (dd, *J* = 241.4, 7.6 Hz), 147.52, 139.63, 139.33, 133.97 (t, *J* = 16.3 Hz), 130.53, 130.22 (t, *J* = 8.3 Hz), 128.98, 128.90, 125.78, 121.42, 119.23, 119.01, 118.95, 110.56 (dd, *J* = 15.5, 7.5 Hz); HRMS (ESI) calcd for $C_{19}H_{11}F_2N_2O_4$ $[M-H]^-$ 369.0692, found 369.0696.

5.1.17 (*E*)-2-(((3-((2-hydroxyphenyl)sulfonyl)phenyl)imino)methyl)-4-nitrophenol (**21o**)

Step 1: (2-methoxyphenyl)(3-nitrophenyl)sulfane (**40**). To a mixture of 1-bromo-3-nitrobenzene **38** (100 mg, 0.50 mmol), $Pd_2(dba)_3$ (11 mg, 0.01 mmol, 0.025 equiv) and Xantphos (14 mg, 0.02 mmol, 0.05 equiv) in dioxane (5 mL) was added DIEA (165 μL, 0.99 mmol, 2 equiv) and 2-methoxybenzenethiol **39** (60 μL, 0.50 mmol, 1 equiv) *via* syringe under N_2 atmosphere. The resulting mixture was stirred at 100°C for 6 h. Upon completion, the reaction mixture was extracted with EA (10 mL × 3). The organic layers were combined, washed with brine, dried over Na_2SO_4, filtered, and concentrated under reduced pressure. The pure product was obtained as a yellow solid (98 mg, 76%) by flash chromatography (Hexane:EA = 20:1, v/v). ^{1}H NMR (400 MHz, $CDCl_3$) δ 8.04 – 7.96 (m, 2H), 7.59 – 7.36 (m, 4H), 7.06 – 6.97 (m, 2H), 3.86 (s, 3H).

Step 2: 2-((3-nitrophenyl)sulfonyl)phenol (**41**). To a solution of **40** (150 mg, 0.57 mmol) in DCM (5 mL) was added *m*-chloroperoxybenzoic acid (218 mg, 1.26 mmol, 2.2 equiv). The resulting mixutre was stirred at room temperature for 1 h. Upon completion, the reaction mixture was quenched by saturated sodium thiosulfate aqueous solution and extracted with DCM (10 mL × 3). The organic layers were combined, washed with saturated $NaHCO_3$ aqueous solution and brine, dried over Na_2SO_4, filtered and concentrated under reduced pressure. The residue was redissolved in anhydrous DCM (10 mL), followed by the addition of aluminum chloride (383 mg, 2.87 mmol, 5 equiv). The resulting solution was stirred at room temperature for 1 h. Upon completion, the reaction mixture was quenched by 1N hydrochloric acid and extracted with DCM (10 mL × 3). The organic layers were combined, washed with brine, dried over Na_2SO_4, filtered and concentrated under reduced pressure. The organic layers

were combined, washed with brine, dried over Na_2SO_4, filtered, concentrated under reduced pressure, and dried *in vacuo* to afford the crude product as a yellow solid (114 mg, 71%), which was used directly in the next step without further purification.

Step 3: 2-((3-aminophenyl)sulfonyl)phenol (**16**). To a solution of **41** (114mg) in a mixture of EtOH/water (7 mL, 5:2, v/v) was added NH_4Cl (154 mg, 2.87 mmol, 5 equiv) and iron powder (160 mg, 2.87 mmol, 5 equiv). The resulting mixture was stirred at 80℃ for 1 h. Upon completion, the reaction mixture was filtered through a short pad of Celite and the filtrate was extracted with EA (10 mL × 3). The organic layers were combined, washed with brine, dried over Na_2SO_4, filtered, concentrated under reduced pressure, and dried *in vacuo* to afford the crude product as a yellow solid (77 mg, 76%), which was used directly in the next step without further purification.

Step 4: The title compound was prepared according to general procedure (**A)** using 5-nitrosalicylaldehyde **1** (60 mg, 0.36 mmol) and **16** (89 mg, 0.36 mmol, 1 equiv), yielding the pure product as a yellow solid (126 mg, 88%). ^{1}H NMR (400 MHz, $CDCl_3$) δ 13.62 (s, 1H), 9.16 (s, 1H), 8.75 (s, 1H), 8.46 (d, J = 2.7 Hz, 1H), 8.34 (dd, J = 9.2, 2.7 Hz, 1H), 7.93 (dt, J = 7.8, 1.3 Hz, 1H), 7.89 (t, J = 2.0 Hz, 1H), 7.72 (dd, J = 8.1, 1.7 Hz, 1H), 7.66 (t, J = 7.9 Hz, 1H), 7.57 – 7.49 (m, 2H), 7.16 (d, J = 9.1 Hz, 1H), 7.08 – 7.00 (m, 2H). ^{13}C NMR (100 MHz, DMSO-d_6) δ 166.3, 163.0, 156.3, 148.5, 143.2, 139.9, 136.4, 130.7, 129.4, 129.1, 128.3, 126.9, 126.8, 126.4, 121.0, 119.7, 119.5, 118.6, 118.0; HRMS (ESI) calcd for $C_{19}H_{13}N_2O_6S$ $[M\text{-}H]^-$ 397.0500, found 397.0503.

5.1.18 (*E*)-2-(([1,1'-biphenyl]-2-ylimino)methyl)-4-nitrophenol (**21p**)

The title compound was prepared according to general procedure (**A)** using 5-nitrosalicylaldehyde **1** (100 mg, 0.60 mmol) and [1,1'-biphenyl]-2-amine **17** (101 mg, 0.60 mmol, 1 equiv), yielding the pure product as a yellow solid (166 mg, 87%). ^{1}H NMR (400 MHz, $CDCl_3$) δ 13.77 (s, 1H), 8.74 (s, 1H), 8.37 (d, *J* = 2.8 Hz, 1H), 8.23 (dd, *J* = 9.2, 2.8 Hz, 1H), 7.55 – 7.38 (m, 8H), 7.35 (d, *J* = 7.6 Hz, 1H), 6.99 (d, *J* = 9.2 Hz, 1H); ^{13}C NMR (100 MHz, $CDCl_3$) δ 166.5, 160.5, 144.5, 139.9, 138.9, 137.6, 131.0, 129.6, 128.8, 128.4, 128.3, 128.3, 128.2, 127.7, 118.3, 118.3, 118.2; HRMS (ESI) calcd for $C_{19}H_{13}N_2O_3$ $[M-H]^-$ 317.0932, found 317.0930.

5.1.19 (*E*)-2-(([1,1'-biphenyl]-3-ylimino)methyl)-4-nitrophenol (**21q**)

The title compound was prepared according to general procedure (**A)** using 5-nitrosalicylaldehyde **1** (100 mg, 0.60 mmol) and [1,1'-biphenyl]-3-amine **18** (101 mg, 0.60 mmol, 1 equiv), yielding the pure product as a yellow solid (150 mg, 79%). ^{1}H NMR (400 MHz, $CDCl_3$) δ 14.46 (s, 1H), 8.81 (s, 1H), 8.44 (d, *J* = 2.7 Hz, 1H), 8.31 (dd, *J* = 9.2, 2.8 Hz, 1H), 7.69 – 7.64 (m, 2H), 7.63 – 7.60 (m, 1H), 7.59 – 7.54 (m, 2H), 7.51 (t, *J* = 7.5 Hz, 2H), 7.43 (t, *J* = 7.3 Hz, 1H), 7.34 (d, *J* = 7.7 Hz, 1H), 7.14 (d, *J* = 9.2 Hz, 1H); ^{13}C NMR (100 MHz, $CDCl_3$) δ 166.9, 160.9, 147.2, 143.0, 140.1, 140.0, 130.1, 129.0, 128.5, 128.4, 128.0, 127.2, 126.8, 120.2, 119.8, 118.4, 118.1; HRMS (ESI) calcd for $C_{19}H_{13}N_2O_3$ $[M-H]^-$ 317.0932, found 317.0930.

5.1.20 (*E*)-2-(([1,1'-biphenyl]-4-ylimino)methyl)-4-nitrophenol (**21r**)

The title compound was prepared according to general procedure (**A)** using 5-

nitrosalicylaldehyde **1** (100 mg, 0.60 mmol) and [1,1'-biphenyl]-4-amine **19** (101 mg, 0.60 mmol, 1 equiv), yielding the pure product as a yellow solid (171 mg, 90%). ^{1}H NMR (400 MHz, $CDCl_3$) δ 14.51 (s, 1H), 8.80 (s, 1H), 8.43 (d, *J* = 2.8 Hz, 1H), 8.30 (dd, *J* = 9.2, 2.8 Hz, 1H), 7.73 (d, *J* = 8.1 Hz, 2H), 7.65 (d, *J* = 7.1 Hz, 2H), 7.50 (t, *J* = 7.5 Hz, 2H), 7.46 – 7.39 (m, 3H), 7.13 (d, *J* = 9.1 Hz, 1H); ^{13}C NMR (100 MHz, DMSO-*d*$_6$) δ 167.4, 161.7, 146.0, 139.9, 139.6, 139.6, 129.5, 128.9, 128.9, 128.2, 128.2, 127.1, 122.5, 119.1, 118.8; HRMS (ESI) calcd for $C_{19}H_{13}N_2O_3$ $[M-H]^-$ 317.0932, found 317.0935.

5.1.21 General procedure (B) for synthesis of amine-linked derivatives

To a solution of Schiff base type derivatives (1 equiv) obtained according to general procedure (**A**) in DCM (10 mL) was added sodium triacetoxyborohydride (3 equiv), and the reaction mixture was stirred at room temperature overnight. Upon completion, the reaction mixture was concentrated under reduced pressure and the pure product was obtained by flash chromatography.

5.1.22 3-((2-hydroxy-5-nitrobenzyl)amino)benzamide (**22a**)

The title compound was prepared according to general procedure (**B**) using **21a** (72 mg, 0.25 mmol), yielding the pure product as a white solid (65 mg, 90%) by flash chromatography (DCM:MeOH = 100:1, v/v). ^{1}H NMR (400 MHz, DMSO-*d*$_6$) δ 11.43 (br s, 1H), 8.07 (d, *J* = 2.9 Hz, 1H), 8.03 (dd, *J* = 8.8, 2.9 Hz, 1H), 7.78 (br s, 1H), 7.17 (br s, 1H), 7.12 (t, *J* = 7.8 Hz, 1H), 7.08 – 7.02 (m, 3H), 6.71 (dd, *J* = 8.1, 2.3 Hz, 1H), 6.43 (br s, 1H), 4.29 (s, 2H); ^{13}C NMR (100 MHz, DMSO-*d*$_6$) δ 169.0, 162.4, 148.8, 139.9, 135.7, 129.2, 127.9, 124.8, 124.0, 115.6,

115.4, 111.6, 41.3; HRMS (ESI) calcd for $C_{14}H_{12}N_3O_4$ $[M-H]^-$ 286.0833, found 286.0833.

5.1.23 3-((2-hydroxy-5-nitrobenzyl)amino)benzenesulfonamide (**22b)**

The title compound was prepared according to general procedure (**B**) using **21b** (65 mg, 0.20 mmol), yielding the pure product as a white solid (55 mg, 84%) by flash chromatography (DCM:MeOH = 100:1, v/v). 1H NMR (400 MHz, DMSO-d_6) δ 11.38 (s, 1H), 8.06 (d, J = 14.7 Hz, 2H), 7.30 – 7.11 (m, 3H), 7.11 – 6.90 (m, 3H), 6.83 – 6.60 (m, 2H), 4.30 (s, 2H); ^{13}C NMR (100 MHz, DMSO-d_6) δ 162.1, 149.1, 145.4, 140.1, 123.0, 127.4, 124.9, 124.0, 115.6, 115.2, 113.4, 109.3, 41.2; HRMS (ESI) calcd for $C_{13}H_{12}N_3O_5S$ $[M-H]^-$ 322.0503, found 322.0501.

5.1.24 2-((2-hydroxy-5-nitrobenzyl)amino)benzonitrile (**22c**)

The title compound was prepared according to general procedure (**B**) using **21c** (65 mg, 0.24 mmol), yielding the pure product as a white solid (61 mg, 93%) by flash chromatography (Hexane:EA = 10:1, v/v). ^{1}H NMR (400 MHz, DMSO-d_6) δ 8.03 – 8.00 (m, 2H), 7.50 (d, J = 7.8 Hz, 1H), 7.35 (t, J = 8.0 Hz, 1H), 6.96 (t, J = 8.1 Hz, 1H), 6.80 (s, 1H), 6.74 – 6.50 (m, 2H), 4.39 (s, 2H); ^{13}C NMR (100 MHz, DMSO-d_6) δ 162.3, 150.5, 140.0, 135.0, 133.8, 126.8, 125.0, 124.1, 118.5, 116.8, 115.8, 111.6, 95.2, 41.0; HRMS (ESI) calcd for $C_{14}H_{10}N_3O_3$ $[M-H]^-$ 268.0728, found 268.0728.

5.1.25 3-((2-hydroxy-5-nitrobenzyl)amino)benzonitrile (**22d**)

The title compound was prepared according to general procedure (**B**) using **21d** (63 mg, 0.24 mmol), yielding the pure product as a white solid (59 mg, 93%) by flash chromatography

(Hexane:EA = 10:1, v/v). ^{1}H NMR (400 MHz, DMSO-*d*$_6$) δ 11.39 (br s, 1H), 8.08 (d, *J* = 2.9 Hz, 1H), 8.05 (dd, *J* = 8.8, 2.9 Hz, 1H), 7.29 – 7.21 (m, 1H), 7.02 (d, *J* = 8.8 Hz, 1H), 6.97 – 6.87 (m, 3H), 6.77 (t, *J* = 6.2 Hz, 1H), 4.29 (d, *J* = 5.7 Hz, 2H); ^{13}C NMR (100 MHz, DMSO-*d*$_6$) δ 162.3, 149.3, 140.0, 130.7, 127.1, 125.0, 124.4, 119.9, 119.7, 117.5, 115.7, 114.4, 112.2, 40.9; HRMS (ESI) calcd for $C_{14}H_{10}N_3O_3$ $[M-H]^-$ 268.0728, found 268.0728.

5.1.26 4-((2-hydroxy-5-nitrobenzyl)amino)benzonitrile (**22e**)

The title compound was prepared according to general procedure (**B**) using **21e** (70 mg, 0.26 mmol), yielding the pure product as a white solid (62 mg, 88%) by flash chromatography (Hexane:EA = 10:1, v/v). ^{1}H NMR (400 MHz, DMSO-*d*$_6$) δ 11.40 (s, 1H), 8.07 – 8.04 (m, 2H), 7.46 (d, *J* = 8.5 Hz, 2H), 7.26 (t, *J* = 6.1 Hz, 1H), 7.02 (d, *J* = 8.5 Hz, 1H), 6.66 (d, *J* = 8.8 Hz, 2H), 4.33 (d, *J* = 6.1 Hz, 2H); ^{13}C NMR (100 MHz, DMSO-*d*$_6$) δ 162.2, 152.3, 140.1, 134.0, 126.7, 125.1, 124.2, 120.9, 115.7, 112.5, 96.8, 40.7; HRMS (ESI) calcd for $C_{14}H_{10}N_3O_3$ $[M-H]^-$ 268.0728, found 268.0728.

5.1.27 2-(3-((2-hydroxy-5-nitrobenzyl)amino)phenyl)acetonitrile (**22f**)

The title compound was prepared according to general procedure (**B**) using **21f** (78 mg, 0.28 mmol), yielding the pure product as a white solid (67 mg, 85%) by flash chromatography (Hexane:EA = 10:1, v/v). ^{1}H NMR (400 MHz, DMSO-*d*$_6$) δ 11.32 (br s, 1H), 8.08 (d, *J* = 2.8 Hz, 1H), 8.03 (dd, *J* = 8.8, 3.0 Hz, 1H), 7.07 (t, *J* = 7.8 Hz, 1H), 7.01 (d, *J* = 8.8 Hz, 1H), 6.57 (s, 1H), 6.51 – 6.49 (m, 2H), 4.26 (s, 2H), 3.87 (s, 2H); ^{13}C NMR (100 MHz, DMSO-*d*$_6$) δ 162.1, 149.3, 140.1, 132.3, 130.1, 127.8, 124.8, 124.1, 119.8, 116.1, 115.6, 112.1, 111.5, 41.1,

23.0; HRMS (ESI) calcd for $C_{14}H_{10}N_3O_3$ $[M-H]^-$ 282.0884, found 282.0884.

5.1.28 2-(3-((2-hydroxy-5-nitrobenzyl)amino)phenyl)acetic acid (**22g**)

The title compound was prepared according to general procedure (**B**) using **21g** (79 mg, 0.26 mmol), yielding the pure product as a white solid (64 mg, 80%) by flash chromatography (DCM:MeOH = 50:1, v/v). ^{1}H NMR (400 MHz, DMSO-d_6) δ 11.91 (br s, 1H), 8.10 (d, J = 2.8 Hz, 1H), 8.03 (dd, J = 9.0, 2.8 Hz, 1H), 7.00 (t, J = 8.4 Hz, 2H), 6.52 (s, 1H), 6.43 (dd, J = 13.0, 7.9 Hz, 2H), 4.24 (s, 2H), 3.39 (s, 2H); ^{13}C NMR (100 MHz, DMSO-d_6) δ 173.2, 162.0, 148.9, 140.1, 136.0, 129.4, 128.1, 124.7, 124.2, 117.7, 115.6, 113.9, 110.6, 41.6, 41.3; HRMS (ESI) calcd for $C_{15}H_{13}N_2O_5$ $[M-H]^-$ 301.0830, found 301.0827.

5.1.29 N-(3-((2-hydroxy-5-nitrobenzyl)amino)benzyl)methanesulfonamide (**22h**)

The title compound was prepared according to general procedure (**B**) using **21h** (79 mg, 0.22 mmol), yielding the pure product as a yellow solid (64 mg, 81%) by flash chromatography (Hexane:EA = 3:1, v/v). ^{1}H NMR (400 MHz, DMSO-d_6) δ 11.30 (s, 1H), 8.07 (d, J = 2.9 Hz, 1H), 8.03 (dd, J = 8.8, 2.9 Hz, 1H), 7.44 (t, J = 6.3 Hz, 1H), 7.07 – 6.98 (m, 2H), 6.59 (d, J = 2.1 Hz, 1H), 6.53 (d, J = 7.5 Hz, 1H), 6.45 (dd, J = 7.9, 2.5 Hz, 1H), 4.26 (s, 2H), 4.00 (d, J = 6.4 Hz, 2H), 2.76 (s, 3H); ^{13}C NMR (100 MHz, DMSO-d_6) δ 162.1, 148.9, 140.1, 139.3, 129.5, 128.1, 124.7, 124.0, 116.0, 115.5, 112.0, 111.3, 46.9, 41.2; HRMS (ESI) calcd for $C_{15}H_{16}N_3O_5S$ $[M-H]^-$ 350.0816, found 350.0818.

5.1.30 4-nitro-2-(((3-(2,2,2-trifluoro-1-hydroxyethyl)phenyl)amino)methyl)phenol (**22i**)

The title compound was prepared according to general procedure (**B**) using **21i** (52 mg, 0.15 mmol), yielding the pure product as a white solid (43 mg, 83%) by flash chromatography (Hexane:EA = 10:1, v/v). ^{1}H NMR (400 MHz, Acetone-d_6) δ 10.20 (br s, 1H), 8.24 (d, J = 2.9 Hz, 1H), 8.06 (dd, J = 2.9, 8.8 Hz, 1H), 7.14 (t, J = 7.8 Hz, 1H), 7.08 (d, J = 8.9 Hz, 1H), 6.93 (s, 1H), 6.81 (d, J = 7.6 Hz, 1H), 6.71 (d, J = 8.2 Hz, 1H), 5.73 (br s, 2H), 5.04 (q, J = 7.3 Hz, 1H), 4.49 (s, 2H); ^{13}C NMR (100 MHz, Acetone-d_6) δ 161.1, 148.4, 140.9, 136.6, 128.9, 127.4, 125.2 (q, J = 280.2 Hz), 124.2, 124.1, 116.5, 115.2, 113.2, 112.3, 72.0 (q, J = 30.9 Hz), 42.1; HRMS (ESI) calcd for $C_{15}H_{12}F_3N_2O_4$ $[M-H]^-$ 341.0755, found 341.0758.

5.1.31 3-((2-hydroxy-5-nitrobenzyl)amino)-*N*-(methylsulfonyl)benzamide (**22j**)

The title compound was prepared according to general procedure (**B**) using **21k** (30 mg, 0.08 mmol), yielding the pure product as a white solid (27 mg, 90%) by flash chromatography (DCM:MeOH = 100:1, v/v). ^{1}H NMR (400 MHz, DMSO-d_6) δ 11.95 (br s, 1H), 11.38 (br s, 1H), 8.14 – 7.96 (m, 2H), 7.21 (td, J = 7.8, 3.1 Hz, 1H), 7.16 – 7.08 (m, 2H), 7.03 (dd, J = 8.8, 3.0 Hz, 1H), 6.85 (d, J = 7.5 Hz, 1H), 6.60 (br s, 1H), 4.32 (s, 2H), 3.36 (s, 3H); ^{13}C NMR (100 MHz, DMSO-d_6) δ 167.4, 162.1, 149.0, 140.1, 133.0, 129.6, 127.6, 124.9, 124.0, 117.5, 116.5, 115.6, 111.7, 41.8, 41.10; HRMS (ESI) calcd for $C_{15}H_{14}N_3O_6S$ $[M-H]^-$ 364.0609, found 364.0605.

5.1.32 *N*-(*N*,*N*-dimethylsulfamoyl)-3-((2-hydroxy-5-nitrobenzyl)amino)benzamide (**22k**)

The title compound was prepared according to general procedure (**B**) using **21l** (47 mg, 0.12 mmol), yielding the pure product as a white solid (36 mg, 76%) by flash chromatography

(DCM:MeOH = 100:1, v/v). ^{1}H NMR (400 MHz, DMSO-d_6) δ 11.59 (br s, 1H), 11.41 (br s, 1H), 8.09 (s, 1H), 8.04 (d, J = 8.7 Hz, 1H), 7.19 (t, J = 7.7 Hz, 1H), 7.11 – 7.09 (m, 2H), 7.02 (d, J = 8.9 Hz, 1H), 6.82 (d, J = 8.2 Hz, 1H), 6.56 (br s, 1H), 4.32 (s, 2H), 2.86 (s, 6H); ^{13}C NMR (100 MHz, DMSO-d_6) δ 166.9, 162.1, 148.9, 140.1, 133.2, 129.6, 127.6, 124.9, 124.1, 117.1, 116.5, 115.6, 111.8, 41.1, 38.4; HRMS (ESI) calcd for $C_{16}H_{17}N_4O_6S$ $[M-H]^-$ 393.0874, found 393.0869.

5.1.33 3-(3-((2-hydroxy-5-nitrobenzyl)amino)phenyl)-1,2,4-oxadiazol-5(4*H*)-one (**22l**)

The title compound was prepared according to general procedure (**B**) using **21m** (34 mg, 0.10 mmol), yielding the pure product as a yellow solid (30 mg, 88%) by flash chromatography (Hexane:EA = 3:1, v/v). ^{1}H NMR (400 MHz, DMSO-d_6) δ 8.07 (d, J = 2.9 Hz, 1H), 8.04 (dd, J = 8.7, 3.0 Hz, 1H), 7.25 (t, J = 7.9 Hz, 1H), 7.02 (d, J = 8.8 Hz, 1H), 7.00 – 6.95 (m, 2H), 6.83 (d, J = 8.0 Hz, 1H), 6.68 (s, 1H), 4.30 (s, 2H). ^{13}C NMR (100 MHz, DMSO-d_6) δ 162.2, 160.8, 158.5, 149.3, 140.1, 130.3, 127.5, 124.9, 124.6, 124.0, 116.6, 115.6, 114.3, 108.8, 41.0; HRMS (ESI) calcd for $C_{15}H_{11}N_4O_5$ $[M-H]^-$ 327.0735, found 327.0737.

5.1.34 3,5-difluoro-3'-((2-hydroxy-5-nitrobenzyl)amino)-[1,1'-biphenyl]-4-ol (**22m**)

The title compound was prepared according to general procedure (**B**) using **21n** (77 mg, 0.21 mmol), yielding the pure product as a yellow solid (66 mg, 85%) by flash chromatography (Hexane:EA = 5:1, v/v). ^{1}H NMR (400 MHz, DMSO-d_6) δ 11.31 (br s, 1H), 10.24 (br s, 1H), 8.14 (s, 1H), 8.03 (d, J = 8.9 Hz, 1H), 7.24 (d, J = 8.5 Hz, 2H), 7.12 (t, J = 7.8 Hz, 1H), 7.02 (d, J = 8.9 Hz, 1H), 6.89 – 6.77 (m, 2H), 6.55 (d, J = 8.1 Hz, 1H), 6.34 (br s, 1H), 4.33 (s, 2H);

^{13}C NMR (100 MHz, DMSO-d_6) δ 162.1, 153.0 (dd, J = 7.7, 241.2 Hz), 149.3, 140.1, 139.2, 133.3 (t, J = 16.3 Hz), 132.1 (t, J = 8.2 Hz), 130.1, 128.0, 124.8, 124.4, 115.6, 114.8, 112.1, 110.3, 110.1 (dd, J = 7.3, 15.2 Hz), 41.2; HRMS (ESI) calcd for $C_{19}H_{13}F_2N_2O_4$ $[M-H]^-$ 371.0849, found 371.0851.

5.1.35 2-(((3-((2-hydroxyphenyl)sulfonyl)phenyl)amino)methyl)-4-nitrophenol (**22n**)

The title compound was prepared according to general procedure (**B**) using **21o** (64 mg, 0.16 mmol), yielding the pure product as a yellow solid (51 mg, 79%) by flash chromatography (Hexane:EA = 5:1, v/v). ^{1}H NMR (400 MHz, DMSO-d_6) δ 10.65 (br s, 1H), 8.03 (d, J = 7.4 Hz, 2H), 7.82 (dd, J = 8.1, 1.7 Hz, 1H), 7.45 (td, J = 7.8, 1.7 Hz, 1H), 7.24 (t, J = 7.9 Hz, 1H), 7.10 (t, J = 2.2 Hz, 1H), 7.02 (ddd, J = 7.5, 5.9, 1.8 Hz, 2H), 6.96 (t, J = 7.6 Hz, 1H), 6.88 (d, J = 8.3 Hz, 1H), 6.82 – 6.77 (m, 2H), 4.26 (s, 2H); ^{13}C NMR (100 MHz, DMSO-d_6) δ 162.1, 156.3, 149.0, 142.6, 140.0, 135.8, 129.9, 129.3, 127.1, 126.8, 124.9, 124.2, 119.3, 117.9, 116.3, 115.7, 115.2, 111.3, 41.1; HRMS (ESI) calcd for $C_{19}H_{15}N_2O_6S$ $[M-H]^-$ 399.0656, found 399.0658.

5.1.36 2-(([1,1'-biphenyl]-2-ylamino)methyl)-4-nitrophenol (**22o**)

The title compound was prepared according to general procedure (**B**) using **21p** (89 mg, 0.28 mmol), yielding the pure product as a white solid (76 mg, 85%) by flash chromatography (Hexane:EA = 10:1, v/v). ^{1}H NMR (400 MHz, $CDCl_3$) δ 10.11 (br s, 1H), 8.18 – 8.07 (m, 2H), 7.51 (t, J = 7.4 Hz, 2H), 7.45 – 7.40 (m, 3H), 7.31 (t, J = 7.3 Hz, 1H), 7.23 (d, J = 7.4 Hz, 1H), 7.07 (t, J = 7.5 Hz, 1H), 6.94 (dd, J = 12.5, 8.4 Hz, 2H), 4.51 (s, 2H), 4.28 (s, 1H); ^{13}C NMR

(100 MHz, $CDCl_3$) δ 163.2, 143.3, 140.8, 138.2, 131.5, 130.6, 129.3, 129.2, 129.0, 128.0, 125.3, 124.4, 123.1, 121.7, 117.1, 114.8, 49.3; HRMS (ESI) calcd for $C_{19}H_{15}N_2O_3$ $[M-H]^-$ 319.1088, found 319.1085.

5.1.37 2-(([1,1'-biphenyl]-3-ylamino)methyl)-4-nitrophenol (**22p**)

The title compound was prepared according to general procedure (**B**) using **21q** (79 mg, 0.25 mmol), yielding the pure product as a white solid (73 mg, 92%) by flash chromatography (Hexane:EA = 10:1, v/v). ^1H NMR (400 MHz, $CDCl_3$) δ 10.01 (br s, 1H), 8.19 – 8.16 (m, 2H), 7.55 (d, J = 7.2 Hz, 2H), 7.46 (t, J = 7.5 Hz, 2H), 7.40 – 7.35 (m, 2H), 7.24 (d, J = 7.8 Hz, 1H), 7.11 (s, 1H), 7.02 – 6.93 (m, 1H), 6.88 (dd, J = 8.1, 2.3 Hz, 1H), 4.62 (s, 2H), 4.19 (s, 1H); ^{13}C NMR (100 MHz, $CDCl_3$) δ 163.2, 146.5, 142.8, 140.8, 140.7, 130.0, 128.9, 127.7, 127.1, 125.5, 124.6, 123.0, 121.0, 117.2, 115.5, 115.2, 49.0; HRMS (ESI) calcd for $C_{19}H_{15}N_2O_3$ $[M-H]^-$ 319.1088, found 319.1089.

5.1.38 2-(([1,1'-biphenyl]-4-ylamino)methyl)-4-nitrophenol (**22q**)

The title compound was prepared according to general procedure (**B**) using **21r** (93 mg, 0.29 mmol), yielding the pure product as a white solid (79 mg, 84%) by flash chromatography (Hexane:EA = 10:1, v/v). ^1H NMR (400 MHz, $CDCl_3$) δ 10.00 (s, 1H), 8.26 – 8.07 (m, 2H), 7.54 (t, J = 8.7 Hz, 4H), 7.44 (t, J = 7.5 Hz, 2H), 7.34 (t, J = 7.4 Hz, 1H), 6.98 – 6.95 (m, 3H), 4.60 (s, 2H), 4.21 (s, 1H); ^{13}C NMR (100 MHz, $CDCl_3$) δ 163.1, 145.4, 140.9, 140.5, 135.0, 128.8, 128.2, 127.0, 126.7, 125.5, 124.6, 123.0, 117.1, 116.8, 49.0; HRMS (ESI) calcd for $C_{19}H_{15}N_2O_3$ $[M-H]^-$ 319.1088, found 319.1091.

5.1.39 4-nitro-2-(((2-(phenylethynyl)phenyl)amino)methyl)phenol (**22r**)

Step 1: 2-(phenylethynyl)aniline (**20**). To a solution of 2-iodoaniline **42** (500 mg, 2.28 mmol) in anhydrous THF (8 mL) was added bis(triphenylphosphine)palladium(II) dichloride (48 mg, 0.07 mmol, 0.03 equiv), copper(I) iodide (22 mg, 0.12 mmol, 0.05 equiv), TEA (2 mL) and phenylacetylene (376 μL, 3.42 mmol, 1.5 equiv) under N_2 atmosphere. The resulting mixture was stirred at room temperature overnight. Upon completion, the reaction mixture was extracted with EA (20 mL × 3). The organic layers were combined, washed with brine, dried over Na_2SO_4, filtered, and concentrated under reduced pressure. The pure product was obtained as a white solid (360 mg, 91%) by flash chromatography (Hexane:EA = 15:1, v/v). ^{1}H NMR (400 MHz, $CDCl_3$) δ 7.62 – 7.49 (m, 2H), 7.43 – 7.31 (m, 4H), 7.17 (td, *J* = 7.7, 1.6 Hz, 1H), 6.75 (t, *J* = 7.4 Hz, 2H), 4.30 (s, 2H).

Step 2: (*E*)-4-nitro-2-(((2-(phenylethynyl)phenyl)imino)methyl)phenol was prepared according to general procedure (**A)** using 5-nitrosalicylaldehyde (50 mg, 0.30 mmol) and **20** (52 mg, 0.30 mmol, 1 equiv), yielding the pure product as a yellow solid (90 mg, 88%), which was subjected to general procedure (**B**) without further purification, yielding the pure product as a white solid (84 mg, 93%) by flash chromatography (Hexane:EA = 10:1, v/v). ^{1}H NMR (400 MHz, $CDCl_3$) δ 9.57 (s, 1H), 8.18 – 8.14 (m, 2H), 7.61 – 7.43 (m, 3H), 7.47 – 7.32 (m, 3H), 7.30 (s, 1H), 6.97 (d, *J* = 8.2 Hz, 2H), 6.85 (d, *J* = 8.2 Hz, 1H), 4.99 (s, 1H), 4.64 (s, 2H); ^{13}C NMR (100 MHz, $CDCl_3$) δ 162.7, 147.2, 141.0, 132.5, 131.6, 130.0, 128.8, 128.5, 125.4, 124.6, 123.2, 122.6, 120.9, 117.1, 113.5, 111.7, 96.2, 84.7, 48.3; HRMS (ESI) calcd for $C_{21}H_{15}N_2O_3$ $[M\text{-}H]^-$ 343.1088, found 343.1090.

5.2 Biology

5.2.1 Determination of minimum inhibitory concentration (MIC)

Antimicrobial activites of all test compounds were assessed by broth microdilution in accordance with the CLSI guidelines [17]. Media used were cation-adjusted Mueller-Hinton broth (CA-MHB) (Oxoid), tryptic-soy broth (TSB) (Oxoid) for staphylococcal-optimized operations, or brain-heart infusion (BHI) (Oxoid) for streptococcal-optimized operations. Two-fold serial dilutions were performed, ranging from 256 μg/mL to 0.25 μg/mL for nusbiarylin test compounds, 64 μg/mL to 0.0625 μg/mL for all antibiotic controls with the exception of rifampicin (2 μg/mL to 1.953125 ng/mL) and linezolid (16 μg/mL to 0.015625 μg/mL). Each bacterial inoculum was adjusted to ~5×10^5 CFU/mL. Results were recorded following 20 hrs of overnight incubation at 37 °C, where MIC was defined as the lowest concentration of antimicrobial compounds eliciting no visible growth in wells. Experiments were performed in triplicates.

5.2.2 Time kill kinetics

The dose- and time-dependent antimicrobial effects of compound **22r** on *S. aureus* strains under aerobic conditions were asseessed by adapting from relevant CLSI guidelines [56]. *Staphylococci* cells at log phase were suspended at ~1.5×10^6 CFU/mL in TSB containing test compounds at predetermined concentrations (i.e. ¼, 1, 4 and 16 MICs) along with untrated controls. Cultures were set-up at 37ºC with agitation at 175 rpm, and 20 μL samples were

retrieved from each treatment group at 0, 2, 4 and 6 hrs and underwent 10-fold serial dilutions in sterile phosphate-buffered saline (PBS). Diluted suspensions were plated onto Columbia blood agar plates and numbers of viable bacterial colonies were counted and expressed as CFU/mL following overnight incubation at 37ºC. Experiments were performed in triplicates.

5.2.3 Assessment of ATP production

Performed in parallel as time-kill kinetics assay, 20 μL samples were taken at identical time points (i.e. 0, 2, 4 and 6 hrs) from the same cultures and placed in white 96-well plates, after which reagents from the BacTiter-Glo™ Microbial Cell Viability Assay Kit (Promega, Madison, Wisconsin, United States) were added at equal volumes. Luminescence readings were taken following the manufacturer's protocol using sterile CA-MHB as background subtraction. The experiment was performed in triplicates.

5.2.4 Serial passage

Fresh colonies of *S. aureus* ATCC® 25923 were obtained by streaking from glycerol stock onto LB agar and incubated overnight at 37 °C. On Day 0, colonies were resuspended in MHB and used to inoculate a broth microdilution plate set up to determine the MIC of **22r** in triplicates according to CLSI guidelines on determining antimicrobial susceptibility. From Day 1 onwards, the latest MIC of **22r** was recorded upon each passage, and the wells containing cells cultured under ¼ MIC of **22r** in each replicate lane were homogenized and used to prepare inoculums for the corresponding fresh replicate lanes. Throughout the assay, each plate was covered with

sterile breathable seals to prevent evaporation and incubated overnight at 37 °C with constant agitation at 180 rpm on an orbital shaker. The process was repeated until its conclusion on Day 12.

5.2.5 Macromolecular quantitation

The effects of varying concentrations of antimicrobials on bacterial DNA, RNA and protein production were characterized by treating *S. aureus* ATCC® 25923 type strain with nusbiarylin compound **22r** and rifampicin at sub-inhibitory concentrations, after which the levels of major macromolecules were quantified. A 100 mL starter culture of *S. aureus* ATCC® 25923 was prepared at OD_{600} 0.1 by inoculating fresh colonies and allowed to grow. Nusbiarylin compound **22r** and rifampicin were added to 17 mL culture aliquots as they reached early log phase (OD_{600} = 0.2) at ¼ and ⅛ MIC levels alongside untreated control. Upon reaching mid-exponential phase (OD_{600} = 0.6), cells were harvested at 3 mL normalized volumes, pelleted at 5000 × *g* for 5 mins, and total DNA, RNA and protein extracted from pellets using the AllPrep® Bacterial DNA/RNA/Protein Kit (Qiagen) following the manufacturer's protocol. In combination with a Qubit 4 Fluorometer (Thermo Fisher), Qubit™ DNA BR Assay Kit (Invitrogen) and Qubit™ RNA BR Assay Kit (Invitrogen) were used to quantify DNA and RNA levels. Pierce BCA Protein Assay Kit (Thermo Fisher) was used to quantify protein concentrations. The experiment was performed in triplicates.

5.2.6 qPCR

To characterise the effects of sub-inhibitory concentrations of antimicrobials on the expression of 16S and 23S ribosomal RNA in comparison with the class drug rifampicin and noramlized against the internal control gene *gyrB* (DNA gyrase B), a starter culture of *S. aureus* ATCC® 25923 was imoculated at OD_{600} 0.1 with fresh colonies and grown to early log phase (~OD_{600} 0.2) at 37 °C with agitation at 175 rpm. Nusbiarylin compound **22r**, along with the rifampicin-containing positive control, were then added at their respective ¼ and ⅛ MICs into aliquots divided from the starter culture alongside an untreated negative control. Upon reaching mid-log phase (~OD_{600} 0.6), approximately 3 mL samples were harvested at normalized volumes and pelleted at 5000 × *g* for 5 mins. After discarding the supernatant, the total RNA was extracted and purified from the pellets using the AllPrep® Bacterial DNA/RNA/Protein Kit (Qiagen), which were then quantified using the Qubit™ RNA BR Assay Kit (Invitrogen) and Qubit 4 Fluorometer (Thermo Fisher).

Purified RNA was then used as template for complementary DNA (cDNA) synthesis using the High-Capacity cDNA Reverse Transcriptino Kit (Applied Biosystems), which were quantified with the Qubit™ ssDNA Assay Kit (Invitrogen). Primer sequences for 16S rRNA, 23S rRNA and DNA gyrase B (*gyrB*), along with their respective sources of design, were listed in **Table 7.**

Table 7. The primers used for qPCR assays in this study.

Primer	**Sequence**	**Reference**
gyrB.MB-F2	CGCAGGCGATTTTACCATTA	[57]
gyrB.MB-R2	GCTTTCGCTAGATCAAAGTCG	[57]
16S_rRNA_F1	GTAGGTGGCAAGCGTTATCC	[58]
16S_rRNA_R1	CGCACATCAGCGTCAG	[58]
PAN23S-F	TCGCTCAACGGATAAAAG	[59]
PAN23S-R	GATGAACCGACATCGAGGTGC	[59]

Primers and cDNA templates were diluted accordingly as recommended by the manufacturer's

protocol of the 2X PowerUp™ SYBR™ Green Master Mix (Applied Biosystems). For every 20 µL reaction loaded in 0.1 mL-sized MicroAmp® Fast 96-Well Reaction Plate (Applied Biosystems), 10 µL of the 2X master mix was added, followed by 2 µL volumes of both forward and reverse primer solutions, 2 µL of cDNA template and 4 µL of nuclease-free water (Ambion). cDNA was not added for no-template control (NTC) reactions and the corresponding volumes re-allocated to nuclease-free water. The loaded plate was sealed and placed onto a StepOnePlus™ Real-Time PCR System (Applied Biosystems) and 40-cycle reactions were performed, completed with melting curves to ensure correct primer hybridisation took place. Experiments were performed in triplicates and results extrapolated were analysed using the $\Delta\Delta C_T$ method.

5.2.7 Epifluorescence microscopy

B. subtilis strain BS61 (NusB-GFP) [15] was grown on LB agar plate containing 5 µg/mL chloramphenicol. A single colony was incubated in LB medium supplemented with 5 µg/mL chloramphenicol at 37 °C until OD600 ~ 0.6. Compound at ⅛, ¼, ½, 1 MIC was then added to the culture and allowed to incubate for further 15 min. 2.5 µL of cell culture was placed onto 1.2% freshly made agarose plate and covered with a coverslip prior to imaging. Nikon Eclipse Ti2-E Live-cell Fluorescence Imaging System equipped with 60×/1.40 oil objective was used to capture the fluorescence images. The fluorescence images were taken under the Bright-field and Wide-field fluorescence modes using Channel 2 (460/470/490/500 nm) through the FITC (525/50) filter. For macromolecular quantitation, *B. subtilis* stain 168 were grown on LB agar

plate overnight and a single colony was inoculated into LB medium. Compound **22r** at ⅛ and ¼ MIC were added to the culture at early log-phase (OD 0.2), and cells were harvested at mid-log phase (OD 0.5) by centrifugation.

5.2.8 Protein complement assay

2-fold dilution of compounds was used starting from 3 mM. 40 µL *N*-LgBiT-NusB (2.5 µM in PBS) was mixed with 20 µL compound in PBS. The mixture was incubated for 10 min at 37 °C. 40 µL C-SmBiT-NusE (2.5 µM in PBS) was then added, followed by incubation for 10 min at 37 °C. After the incubation step, 100 µL of Promega Nano-Glo® Luciferase Assay Substrate was added to the reaction mixture. Luminescence was measured using a Victor X3 Multilabel plate reader. Experiment was performed in triplicate.

5.2.9 *In vitro* cytotoxicity

Lung carcinoma cell lines A549 and immortalized human keratinocytes HaCaT were used to assess the cytotoxicity of antimicrobial compounds and assay was performed as previously described [14]. On Day 0, cells were seeded at 2.5×10^5 per well in a 96-well plate. Following 24 hrs overnight incubation at 37ºC, test compounds and the positive control cisplatin were added in two-fold serial dilutions ranging from 1.562 mg/mL to 50 µg/mL. Plates were then incubated at 37 °C, and MTT assay was performed at 48 hrs and 72 hrs following addition of compounds to determine cell viability. Results were presented as 50% cytotoxic concentraiont

(CC_{50}) values alongside their respective standard deviations, referring to concentration of compound that reduced cell viability by 50% compared to untreated control.

5.3 Molecular docking

Compounds **MC4-2**, **MC4-6** and **22r** were imported into Discovery Studio 2016 for docking studies. The protonation state of the molecule was determined according to the Henderson-Hasselbalch equation, where $[HA]/[A^-] = 10^{(pK_a-pH)}$ [60]. Subsequently, Prepare Ligands and Minimize Ligands modules of Discovery Studio 2016 were conducted on compounds **MC4-2**, **MC4-6** and **22r.** All the possible energy-minimized conformations were obtained via CHARMm force field. The NusB protein (PDB ID: 3D3B) was chosen for docking studies. SBD_Site_Sphere was centred around the three hot-spot residues (radius = 6.0 Å), which completely covered the NusB binding cavity. Libdock module of Discovery Studio 2016 was used to dock compounds **MC4-2**, **MC4-6** and **22r** into the NusB binding groove under the default rigid docking protocol, with the docking tolerance set to 0.55. Multiple poses were generated and ranked based upon the Libdock scores. Finally, the poses with the highest Libdock scores were chosen as the optimal poses to proceed.

Notes

The authors declare no competing financial interest.

Acknowledgement

The research was supported by Hong Kong RGC General Research Fund No. PolyU 15100019

and C5008-19G (C.M.), Hong Kong Polytechnic University (1-ZE2E and State Key Laboratory of Chemical Biology and Drug Discovery to C.M.), Hong Kong RGC General Research Fund GRF No. CUHK 14100120 (X.Y.), Hong Kong Food and Health Bureau HMRF Grant No. 20190032, Hong Kong (X.Y.) and Chinese University of Hong Kong, Faculty of Medicine Faculty Innovation Award FIA2018/A/03, Hong Kong (X.Y.). We thank the technical support from the University Research Facility of Life Sciences and the University Research Facility in Chemical and Environmental Analysis. We thank Prof. Jinyi Xu of China Pharmaceutical University for the assistance on *in silico* ADME study.

Abbreviations

PPI

protein-protein interaction

SAR

structure-activity relationship

MRSA

methicillin-resistant *Staphylococcus aureus*

VRSA

vancomycin-resistance *Staphylococcus aureus*

MIC

minimum inhibitory concentration

RNAP

RNA polymerase

Boc

tert-butyloxycarbonyl

TFA

trifluoroacetic acid

CLSI

Clinical & Laboratory Standards Institute

MHB

Mueller-Hinton broth

TI

therapeutic index

EA

ethyl acetate

DCM

dichloromethane

DMAP

4-dimethylaminopyridine

DIEA

N,N-diisopropylethylamine

EDC

1-ethyl-3-(3-dimethylaminopropyl)carbodiimide

TEA

triethylamine

References

[1] C. Ma, X. Yang, P.J. Lewis, Bacterial Transcription as a Target for Antibacterial Drug Development, Microbiol Mol Biol Rev, 80 (2016) 139-160.

[2] R. Kahan, D.J. Worm, G.V. de Castro, S. Ng, A. Barnard, Modulators of protein-protein interactions as antimicrobial agents, RSC Chem Biol, 2 (2021) 387-409.

[3] G. Baniulyte, N. Singh, C. Benoit, R. Johnson, R. Ferguson, M. Paramo, A.M. Stringer, A. Scott, P. Lapierre, J.T. Wade, Identification of regulatory targets for the bacterial Nus factor complex, Nat Commun, 8 (2017) 2027.

[4] R. Das, S. Loss, J. Li, D.S. Waugh, S. Tarasov, P.T. Wingfield, R.A. Byrd, A.S. Altieri,

Structural biophysics of the NusB:NusE antitermination complex, J Mol Biol, 376 (2008) 705-720.

[5] J.R. Stagno, A.S. Altieri, M. Bubunenko, S.G. Tarasov, J. Li, D.L. Court, R.A. Byrd, X. Ji, Structural basis for RNA recognition by NusB and NusE in the initiation of transcription antitermination, Nucleic Acids Res, 39 (2011) 7803-7815.

[6] B.M. Burmann, X. Luo, P. Rosch, M.C. Wahl, M.E. Gottesman, Fine tuning of the E. coli NusB:NusE complex affinity to BoxA RNA is required for processive antitermination, Nucleic Acids Res, 38 (2010) 314-326.

[7] S.J. Greive, A.F. Lins, P.H. von Hippel, Assembly of an RNA-protein complex. Binding of NusB and NusE (S10) proteins to boxA RNA nucleates the formation of the antitermination complex involved in controlling rRNA transcription in Escherichia coli, J Biol Chem, 280 (2005) 36397-36408.

[8] H. Luttgen, R. Robelek, R. Muhlberger, T. Diercks, S.C. Schuster, P. Kohler, H. Kessler, A. Bacher, G. Richter, Transcriptional regulation by antitermination. Interaction of RNA with NusB protein and NusB/NusE protein complex of Escherichia coli, J Mol Biol, 316 (2002) 875-885.

[9] N. Said, F. Krupp, E. Anedchenko, K.F. Santos, O. Dybkov, Y.H. Huang, C.T. Lee, B. Loll, E. Behrmann, J. Burger, T. Mielke, J. Loerke, H. Urlaub, C.M.T. Spahn, G. Weber, M.C. Wahl, Structural basis for lambdaN-dependent processive transcription antitermination, Nat Microbiol, 2 (2017) 17062.

[10] D.L. Court, T.A. Patterson, T. Baker, N. Costantino, X. Mao, D.I. Friedman, Structural and functional analyses of the transcription-translation proteins NusB and NusE, J Bacteriol,

177 (1995) 2589-2591.

[11] Y.H. Huang, T. Hilal, B. Loll, J. Burger, T. Mielke, C. Bottcher, N. Said, M.C. Wahl, Structure-Based Mechanisms of a Molecular RNA Polymerase/Chaperone Machine Required for Ribosome Biosynthesis, Mol Cell, 79 (2020) 1024-1036 e1025.

[12] X. Luo, H.H. Hsiao, M. Bubunenko, G. Weber, D.L. Court, M.E. Gottesman, H. Urlaub, M.C. Wahl, Structural and functional analysis of the E. coli NusB-S10 transcription antitermination complex, Mol Cell, 32 (2008) 791-802.

[13] X. Yang, M.J. Luo, A.C.M. Yeung, P.J. Lewis, P.K.S. Chan, M. Ip, C. Ma, First-In-Class Inhibitor of Ribosomal RNA Synthesis with Antimicrobial Activity against Staphylococcus aureus, Biochemistry, 56 (2017) 5049-5052.

[14] Y. Qiu, S.T. Chan, L. Lin, T.L. Shek, T.F. Tsang, N. Barua, Y. Zhang, M. Ip, P.K. Chan, N. Blanchard, G. Hanquet, Z. Zuo, X. Yang, C. Ma, Design, synthesis and biological evaluation of antimicrobial diarylimine and -amine compounds targeting the interaction between the bacterial NusB and NusE proteins, Eur J Med Chem, 178 (2019) 214-231.

[15] Y. Qiu, S.T. Chan, L. Lin, T.L. Shek, T.F. Tsang, Y. Zhang, M. Ip, P.K. Chan, N. Blanchard, G. Hanquet, Z. Zuo, X. Yang, C. Ma, Nusbiarylins, a new class of antimicrobial agents: Rational design of bacterial transcription inhibitors targeting the interaction between the NusB and NusE proteins, Bioorg Chem, 92 (2019) 103203.

[16] A.J. Chu, Y. Qiu, R. Harper, L. Lin, C. Ma, X. Yang, Nusbiarylins Inhibit Transcription and Target Virulence Factors in Bacterial Pathogen Staphylococcus aureus, Int J Mol Sci, 21 (2020).

[17] J. Ye, A.J. Chu, L. Lin, X. Yang, C. Ma, First-In-Class Inhibitors Targeting the Interaction

between Bacterial RNA Polymerase and Sigma Initiation Factor Affect the Viability and Toxin Release of Streptococcus pneumoniae, Molecules, 24 (2019).

[18] J. Ye, A.J. Chu, R. Harper, S.T. Chan, T.L. Shek, Y. Zhang, M. Ip, M. Sambir, I. Artsimovitch, Z. Zuo, X. Yang, C. Ma, Discovery of Antibacterials That Inhibit Bacterial RNA Polymerase Interactions with Sigma Factors, J Med Chem, 63 (2020) 7695-7720.

[19] J. Ye, A.J. Chu, L. Lin, S.T. Chan, R. Harper, M. Xiao, I. Artsimovitch, Z. Zuo, C. Ma, X. Yang, Benzyl and benzoyl benzoic acid inhibitors of bacterial RNA polymerase-sigma factor interaction, Eur J Med Chem, 208 (2020) 112671.

[20] G.A. Patani, E.J. LaVoie, Bioisosterism: A Rational Approach in Drug Design, Chem Rev, 96 (1996) 3147-3176.

[21] P.J. Hajduk, M. Bures, J. Praestgaard, S.W. Fesik, Privileged molecules for protein binding identified from NMR-based screening, J Med Chem, 43 (2000) 3443-3447.

[22] C. Lamberth, J. Dinges, Different Roles of Carboxylic Functions in Pharmaceuticals and Agrochemicals, in: Bioactive Carboxylic Compound Classes: Pharmaceuticals and Agrochemicals, 2016, pp. 1-11.

[23] P. Lassalas, B. Gay, C. Lasfargeas, M.J. James, V. Tran, K.G. Vijayendran, K.R. Brunden, M.C. Kozlowski, C.J. Thomas, A.B. Smith, 3rd, D.M. Huryn, C. Ballatore, Structure Property Relationships of Carboxylic Acid Isosteres, J Med Chem, 59 (2016) 3183-3203.

[24] M. Bandini, A. Gualandi, M. Monari, A. Romaniello, D. Savoia, M. Tragni, Allylic alcohols: Valuable synthetic equivalents of non-activated alkenes in gold-catalyzed enantioselective alkylation of indoles, Journal of Organometallic Chemistry, 696 (2011) 338-347.

[25] H.D. Tagad, Y. Hamada, J.T. Nguyen, T. Hamada, H. Abdel-Rahman, A. Yamani, A. Nagamine, H. Ikari, N. Igawa, K. Hidaka, Y. Sohma, T. Kimura, Y. Kiso, Design of pentapeptidic BACE1 inhibitors with carboxylic acid bioisosteres at P1' and P4 positions, Bioorg Med Chem, 18 (2010) 3175-3186.

[26] I.C. Choong, W. Lew, D. Lee, P. Pham, M.T. Burdett, J.W. Lam, C. Wiesmann, T.N. Luong, B. Fahr, W.L. DeLano, R.S. McDowell, D.A. Allen, D.A. Erlanson, E.M. Gordon, T. O'Brien, Identification of potent and selective small-molecule inhibitors of caspase-3 through the use of extended tethering and structure-based drug design, J Med Chem, 45 (2002) 5005-5022.

[27] C.L.S. Institute, Performance Standards for Antimicrobial Susceptibility Testing, 30th ed., Clinical & Laboratory Standards Institute, Wayne, PA, 2020.

[28] G.W. Kaatz, S.M. Seo, Inducible NorA-mediated multidrug resistance in Staphylococcus aureus, Antimicrob Agents Chemother, 39 (1995) 2650-2655.

[29] J.I. Ross, E.A. Eady, J.H. Cove, S. Baumberg, Minimal functional system required for expression of erythromycin resistance by msrA in Staphylococcus aureus RN4220, Gene, 183 (1996) 143-148.

[30] A.D. Khosravi, A. Jenabi, E.A. Montazeri, Distribution of genes encoding resistance to aminoglycoside modifying enzymes in methicillin-resistant Staphylococcus aureus (MRSA) strains, Kaohsiung J Med Sci, 33 (2017) 587-593.

[31] W. Balemans, L. Vranckx, N. Lounis, O. Pop, J. Guillemont, K. Vergauwen, S. Mol, R. Gilissen, M. Motte, D. Lancois, M. De Bolle, K. Bonroy, H. Lill, K. Andries, D. Bald, A. Koul, Novel antibiotics targeting respiratory ATP synthesis in Gram-positive pathogenic bacteria, Antimicrob Agents Chemother, 56 (2012) 4131-4139.

[32] M.A. Lobritz, P. Belenky, C.B. Porter, A. Gutierrez, J.H. Yang, E.G. Schwarz, D.J. Dwyer, A.S. Khalil, J.J. Collins, Antibiotic efficacy is linked to bacterial cellular respiration, Proc Natl Acad Sci U S A, 112 (2015) 8173-8180.

[33] J.H. Yang, S.C. Bening, J.J. Collins, Antibiotic efficacy-context matters, Curr Opin Microbiol, 39 (2017) 73-80.

[34] L. Hamouche, L. Poljak, A.J. Carpousis, Ribosomal RNA degradation induced by the bacterial RNA polymerase inhibitor rifampicin, RNA, (2021).

[35] J. Ye, L. Lin, J. Xu, P.K. Chan, X. Yang, C. Ma, Design, Synthesis, Biological Evaluation and In Silico Studies of Pyrazole-Based NH2-Acyl Oseltamivir Analogues as Potent Neuraminidase Inhibitors, Pharmaceuticals (Basel), 14 (2021).

[36] J. Ye, X. Yang, M. Xu, P.K. Chan, C. Ma, Novel N-Substituted oseltamivir derivatives as potent influenza neuraminidase inhibitors: Design, synthesis, biological evaluation, ADME prediction and molecular docking studies, Eur J Med Chem, 182 (2019) 111635.

[37] S. Bereswill, H. Bai, G. Sang, Y. You, X. Xue, Y. Zhou, Z. Hou, J. Meng, X. Luo, Targeting RNA Polymerase Primary σ70 as a Therapeutic Strategy against Methicillin-Resistant Staphylococcus aureus by Antisense Peptide Nucleic Acid, PLoS ONE, 7 (2012).

[38] K. Husecken, M. Negri, M. Fruth, S. Boettcher, R.W. Hartmann, J. Haupenthal, Peptide-based investigation of the Escherichia coli RNA polymerase sigma(70):core interface as target site, ACS Chem Biol, 8 (2013) 758-766.

[39] D.S. Wenholz, M. Zeng, C. Ma, M. Mielczarek, X. Yang, M. Bhadbhade, D.S.C. Black, P.J. Lewis, R. Griffith, N. Kumar, Small molecule inhibitors of bacterial transcription complex formation, Bioorg Med Chem Lett, 27 (2017) 4302-4308.

[40] M. Mielczarek, R.V. Thomas, C. Ma, H. Kandemir, X. Yang, M. Bhadbhade, D.S. Black, R. Griffith, P.J. Lewis, N. Kumar, Synthesis and biological activity of novel mono-indole and mono-benzofuran inhibitors of bacterial transcription initiation complex formation, Bioorg Med Chem, 23 (2015) 1763-1775.

[41] H. Kandemir, C. Ma, S.K. Kutty, D.S. Black, R. Griffith, P.J. Lewis, N. Kumar, Synthesis and biological evaluation of 2,5-di(7-indolyl)-1,3,4-oxadiazoles, and 2- and 7-indolyl 2-(1,3,4-thiadiazolyl)ketones as antimicrobials, Bioorg Med Chem, 22 (2014) 1672-1679.

[42] M. Mielczarek, R.V. Devakaram, C. Ma, X. Yang, H. Kandemir, B. Purwono, D.S. Black, R. Griffith, P.J. Lewis, N. Kumar, Synthesis and biological activity of novel bis-indole inhibitors of bacterial transcription initiation complex formation, Org Biomol Chem, 12 (2014) 2882-2894.

[43] E. Andre, L. Bastide, P. Villain-Guillot, J. Latouche, J. Rouby, J.P. Leonetti, A multiwell assay to isolate compounds inhibiting the assembly of the prokaryotic RNA polymerase, Assay Drug Dev Technol, 2 (2004) 629-635.

[44] E. Andre, L. Bastide, S. Michaux-Charachon, A. Gouby, P. Villain-Guillot, J. Latouche, A. Bouchet, M. Gualtieri, J.P. Leonetti, Novel synthetic molecules targeting the bacterial RNA polymerase assembly, J Antimicrob Chemother, 57 (2006) 245-251.

[45] S. Sartini, E. Levati, M. Maccesi, M. Guerra, G. Spadoni, S. Bach, M. Benincasa, M. Scocchi, S. Ottonello, S. Rivara, B. Montanini, New Antimicrobials Targeting Bacterial RNA Polymerase Holoenzyme Assembly Identified with an in Vivo BRET-Based Discovery Platform, ACS Chem Biol, 14 (2019) 1727-1736.

[46] O. Thach, M. Mielczarek, C. Ma, S.K. Kutty, X. Yang, D.S. Black, R. Griffith, P.J. Lewis,

N. Kumar, From indole to pyrrole, furan, thiophene and pyridine: Search for novel small molecule inhibitors of bacterial transcription initiation complex formation, Bioorg Med Chem, 24 (2016) 1171-1182.

[47] C. Ma, M. Mobli, X. Yang, A.N. Keller, G.F. King, P.J. Lewis, RNA polymerase-induced remodelling of NusA produces a pause enhancement complex, Nucleic Acids Res, 43 (2015) 2829-2840.

[48] X. Yang, C. Ma, P. Lewis, A vector system that allows simple generation of mutant Escherichia coli RNA polymerase, Plasmid, 75 (2014) 37-41.

[49] X. Yang, S. Molimau, G.P. Doherty, E.B. Johnston, J. Marles-Wright, R. Rothnagel, B. Hankamer, R.J. Lewis, P.J. Lewis, The structure of bacterial RNA polymerase in complex with the essential transcription elongation factor NusA, EMBO Rep, 10 (2009) 997-1002.

[50] T.F. Tsang, Y. Qiu, L. Lin, J. Ye, C. Ma, X. Yang, Simple Method for Studying in Vitro Protein-Protein Interactions Based on Protein Complementation and Its Application in Drug Screening Targeting Bacterial Transcription, ACS Infect Dis, 5 (2019) 521-527.

[51] X. Yang, C. Ma, P.J. Lewis, Identification of inhibitors of bacterial RNA polymerase, Methods, 86 (2015) 45-50.

[52] X. Yang, C. Ma, In Vitro Transcription Assays and Their Application in Drug Discovery, J Vis Exp, (2016).

[53] C. Ma, X. Yang, H. Kandemir, M. Mielczarek, E.B. Johnston, R. Griffith, N. Kumar, P.J. Lewis, Inhibitors of bacterial transcription initiation complex formation, ACS Chem Biol, 8 (2013) 1972-1980.

[54] C. Ma, X. Yang, P.J. Lewis, Bacterial Transcription Inhibitor of RNA Polymerase

Holoenzyme Formation by Structure-Based Drug Design: From in Silico Screening to Validation, ACS Infect Dis, 2 (2016) 39-46.

[55] Y. Qiu, C. Ma, HPLC, quantitative NMR and HRMS spectroscopic data of nusbiarylins as a new class of antimicrobial agents, Data Brief, 29 (2020) 105313.

[56] C.L.S. Institute, Methods for Dilution Antimicrobial Susceptibility Tests for Bacteria That Grow Aerobically, 11th ed., Clinical & Laboratory Standards Institute, Wayne, PA, 2018.

[57] K. Seidl, L. Chen, A.S. Bayer, W.A. Hady, B.N. Kreiswirth, Y.Q. Xiong, Relationship of agr expression and function with virulence and vancomycin treatment outcomes in experimental endocarditis due to methicillin-resistant Staphylococcus aureus, Antimicrob Agents Chemother, 55 (2011) 5631-5639.

[58] S.R. Monday, G.A. Bohach, Use of multiplex PCR to detect classical and newly described pyrogenic toxin genes in staphylococcal isolates, J Clin Microbiol, 37 (1999) 3411-3414.

[59] P. Gaibani, M. Mariconti, G. Bua, S. Bonora, D. Sassera, M.P. Landini, P. Mulatto, S. Novati, C. Bandi, V. Sambri, Development of a broad-range 23S rDNA real-time PCR assay for the detection and quantification of pathogenic bacteria in human whole blood and plasma specimens, Biomed Res Int, 2013 (2013) 264651.

[60] L. Di, E. Kerns, Drug-like properties: concepts, structure design and methods from ADME to toxicity optimization, Academic press, 2015.